JPL PUBLICATION 81-36

Entrainment and Thrust Augmentation in Pulsatile Ejector Flows

V. Sarohia
L. Bernal
T. Bui

August 15, 1981

Prepared for
Naval Air Systems Command
through an agreement with
National Aeronautics and Space Administration
by
Jet Propulsion Laboratory
California Institute of Technology
Pasadena, California

JPL PUBLICATION 81-36

Entrainment and Thrust Augmentation in Pulsatile Ejector Flows

V. Sarohia
L. Bernal
T. Bui

August 15, 1981

Prepared for
Naval Air Systems Command
through an agreement with
National Aeronautics and Space Administration
by
Jet Propulsion Laboratory
California Institute of Technology
Pasadena, California

The research described in this publication was carried out by the Jet Propulsion Laboratory, California Institute of Technology, and was sponsored by the Naval Air Systems Command through an agreement with NASA.

ABSTRACT

An experimental investigation of axisymmetric subsonic ejector flow with a time-varying primary mass flow rate was undertaken to determine the influence of entrainment and mixing on the augmentation in pulsatile ejector flows. This study comprised direct thrust measurements, flow visualization by use of a spark shadowgraph technique, and mean and fluctuating velocity measurements with a pitot tube and linearized constant temperature hot-wire anemometry respectively. A gain in thrust of as much as 10 to 15% was observed for the pulsatile ejector flow as compared to the steady flow configuration. Except for Strouhal number less than 0.05, this improvement in ejector performance was independent of the frequency of pulsations but was directly proportional to its amplitude. From the velocity profile measurements, it was concluded that this enhanced augmentation for pulsatile flow as compared to a nonpulsatile one was accomplished by a corresponding increased entrainment by the primary jet flow. From this study, it was further concluded that the augmentation and total entrainment by a constant area ejector critically depends upon the inlet geometry of the ejector. Experiments were also performed to evaluate the influence of primary jet to ejector area ratio, ejector length, and presence of a diffuser on pulsatile ejector performance.

TABLE OF CONTENTS

Section	Title	Page
	Abstract	iii
	Table of Contents	v
	List of Tables	vi
	Figure Captions	vii
	Nomenclature	ix
I	Introduction	1
II	Experimental Facilities and Instrumentation	2
III	Experimental Results and Discussion	4
	3.1 Flow Visualization	4
	3.2 Influence of Pulsations on Free-Jet Growth	5
	3.3 Ejector Performance	6
	3.3.1 Thrust Measurement	7
	3.3.2 Entrainment Results	8
	3.3.3 Pressure Distribution	8
	3.3.4 Ejector Length and Area Ratio Effects	9
	3.3.5 Diffuser Effects	9
	3.3.6 Inlet Effects	9
IV	Conclusions	10
	Acknowledgements	10
	References	12
	Tables	14-18
	Figures	19-43

LIST OF TABLES

	Page
Table 1 - Dimensions of the Ejector System	14
Table 2 - Ejector Performance at Various Exit Mach Numbers	15
Table 3 - Influence of the Frequency of Pulsations on Ejector Performance	16
Table 4 - Influence of the Amplitude of Velocity Pulsations on Ejector Performance	17
Table 5 - Influence of Pulsations on Entrainment	18

FIGURE CAPTIONS

		Page
Figure 1.	Schematic Diagram of Thrust Augmentor	19
Figure 2.	Primary Nozzle Flow Experimental Arrangements	20
Figure 3.	Primary Flow and Constant-Area Ejector	21
Figure 4.	Subsonic Jet Exhausting Into Ambient Air Without Upstream Pulsations. Velocity at Nozzle Exit = 52 m/s	22
Figure 5.	Subsonic Jet Exhausting Into Ambient Air With Upstream Pulsations. Velocity at Nozzle Exit = 52 m/s. Frequency $fd/U_e = 0.3$	23
Figure 6.	Shadowgraph Showing Entrained Flow of a Jet. Velocity at Nozzle Exit = 152 m/s	24
Figure 7.	Shadowgraph Showing Entrained Flow of a Pulsed Jet. Nozzle Exit Velocity = 152 m/s. Frequency $fd/U_e = 0.07$	25
Figure 8.	Linearized Constant Temperature Hot-Wire Anemometry Output	26
Figure 9.	Centerline Velocity Decay	27
Figure 10.	Growth of Jet	28
Figure 11.	Entrainment of Flow by a Free-Jet	29
Figure 12.	Conservation of Momentum/Thrust Without Pulsations	30
Figure 13.	Conservation of Momentum/Thrust With Pulsations; f = 54 Hz	31
Figure 14.	Conservation of Momentum/Thurst With Pulsations; f = 136 Hz	32
Figure 15.	Conservation of Momentum/Thrust With Pulsations; f = 273 Hz	33
Figure 16.	Conservation of Momentum/Thrust With Pulsations; f = 546 Hz	34
Figure 17.	Conservation of Momentum/Thrust With Pulsations; f = 819 Hz	35
Figure 18.	Thrust Augmentation of a Constant-Area Ejector	36
Figure 19.	Influence of Amplitude of Velocity Fluctuations on Ejector Performance	37
Figure 20.	Pressure Distribution Along Ejector Wall With and Without Pulsating Primary Jet	38
Figure 21.	Influence of Pulsations on Ejector Performance	39
Figure 22.	Effect of Pulsations on Ejector Performance	40

FIGURE CAPTIONS (Continued)

Page

Figure 23. Effect of Pulsations on Ejector Performance with Diffuser 41

Figure 24. Ejector Inlet Effects 42

Figure 25. Influence of Ejector Inlet Flow on Entrainment 43

NOMENCLATURE

b	width of the jet
$C_p \equiv$	$\frac{P - P_\infty}{1/2 \rho U_e^2}$, pressure coefficient
d	primary nozzle diameter
D	constant-area ejector diameter
D'	inlet diameter of the constant-area ejector (see figure in Table 1)
f	frequency of pulsations
L	length of ejector
L'	length of diffuser
M_e	nozzle exit flow Mach number
p	static pressure
p_∞	ambient pressure
p_0	stagnation pressure
$Q(x)$	volume flow at distance x
Q_e	volume flow at nozzle exit plane (primary jet)
$Re \equiv$	$\frac{\rho U d}{\mu}$
$S \equiv$	$\frac{fd}{U_e}$, nondimensional frequency
T	thrust
T_0	primary nozzle thrust without pulsation
T_0'	primary nozzle thrust with pulsation
u'	longitudinal velocity fluctuation
U	longitudinal mean velocity
u_e	nozzle exit flow velocity
X	longitudinal distance from nozzle exit plane

α	diffuser angle
ρ	gas density
μ	gas viscosity

I. INTRODUCTION

The achievement of high thrust augmentation from an engine exhaust jet ejector system is governed by certain fluid mechanics phenomena associated with the entrainment of surrounding atmospheric air by the primary jet flow and the subsequent mixing of this entrained fluid with the primary jet. These fundamental processes that govern the ejector performance are as yet not adequately understood. The results presented in this report focus on determining the mechanism of primary jet entrainment and mixing and the role of entrainment and mixing in associated thrust augmentation of a fluid ejector.

Furthermore, for the application of thrust ejectors for an aircraft, it is very essential to build a compact and lightweight thrust augmentor system. One of the concepts to enhance the thrust augmentor performance is the utilization of a pulsatile primary jet. Though there are numerous studies performed on steady state ejector flow systems,[1-5] very little is known about mixing processes of the entrained fluid by a pulsatile primary jet flow. Experimental investigations by Binder and Favre-Marinet,[6] Bremhorst, K. and Harch, W.H.,[7] Crow and Champagne,[8] Leister,[9] Platzer, et al.[10] and Wygnanski et al.[11] have demonstrated without doubt the importance of organizing the jet with large-scale structures in order to achieve increased rate of jet growth and hence, increased entrainment of ambient fluid. The growth and entrainment of the jet, however, will be greatly modified by the presence of the ejector because of the imposed pressure field. This pressure field for a pulsating primary jet will depend upon frequency and amplitude of pulsations, an area ratio of primary to secondary flow, and the length of the ejector. The presence of a diffuser will further modify the axial pressure distribution and consequently the growth of the pulsatile primary jet. As yet, very little is

known about the mixing process of the entrained fluid by a pulsatile primary jet as a function of area ratio and the length of the ejector. These are some of the questions which have been addressed in the present investigation.

II. EXPERIMENTAL FACILITIES AND INSTRUMENTATION

To determine the achievable entrainment and mixing of a pulsating primary jet in an ejector configuration as well as ejector performance, controlled experiments were conducted in the setup shown in Figures 1, 2 and 3. Subsonic jet flow was generated by expanding air at room stagnation temperature through an axisymmetric convergent nozzle which has an exit diameter d of 2.54 cm. The flow in the plenum chamber entered at 90° to the axis of the nozzle without contributing to the thrust of the system. As sketched in Figure 1, the flow before entering the plenum chamber could be modulated from frequencies of 20 to 1500 Hz by first passing the flow through a pneumatic transducer. The time-varying primary jet velocity profile (complete jet flow) was achieved by utilizing this pneumatic transducer. To avoid any changes in the mean mass flow rate which may result by the introduction of these modulations, a choked flow condition was maintained in the air supply line upstream of the pneumatic transducer.

The primary nozzle flow system with an area ratio of 25:1 between the plenum chamber and the nozzle exit diameter was carefully designed to avoid any flow separation in the contraction section. Static pressures in the plenum chamber and at the nozzle exit along with their area ratio and gas stagnation temperature were utilized to compute the nozzle exit Mach number. A primary nozzle flow efficiency of 97% (ratio of direct thrust measurement to the thrust for an isentropic expansion) was measured.

A standard constant area ejector with hemispherical nose and with an internal diameter D = 8.9 cm and an external diameter of 17.8 cm with length L

• 30.5 cm was extensively utilized in the present measurements. As indicated in Figures 1 to 3, the ejector system was mounted on a thrust stand where a direct thrust measurement was made with a load-cell. The gap between the primary nozzle and ejector inlet could be varied continuously up to a maximum of 5 primary nozzle diameters. The dimensions of the ejector system for determining the influence of area ratio D/d, ejector length L/D, and the presence of a diffuser are shown in Table 1.

To determine the influence of initial conditions on ejector performance, velocity profiles and thrust measurements were made with no inlet, a flat plate inlet and hemispherical inlets of two different dimensions. These measurements were made in the presence of a standard constant-area ejector system.

To further enhance our understanding of the role of entrained fluid and its consequent mixing with the primary jet, extensive static pressure measurements on the hemispherical nose cone as well as along the length of the ejector were made. The pressure distribution was measured for both nonpulsated and pulsated primary jet flow conditions over a range of flow and frequencies of pulsations.

Constant temperature hot-wire anemometry was utilized to determine the mean and the fluctuating velocity components of the pulsating jet. The data was plotted on x-y plotters and subsequently digitized and processed on the minicomputer data acquisition facility.

The jet flow was visualized by injecting CO_2 gas into the plenum chamber of the nozzle air supply. Still shadowgraphs were taken with a spark source that had a time duration of approximately 1.0 μs. Visualization of the entrained fluid alone was also made by taking spark shadowgraphs of a sheet of fluid marked with CO_2 gas. These results of flow visualization are discussed in the following section.

III. EXPERIMENTAL RESULTS AND DISCUSSION

3.1. Flow Visualization

Spark shadowgraphs showing the jet growth without and with upstream pulsations are shown in Figures 4 and 5 respectively. The Reynolds number based on the nozzle exit diameter and mean velocity was $R_e = 0.9 \times 10^5$. In Figures 4 and 5, in which the mean mass flow rates were equal, and the spreading angle of the jet is significantly enhanced by the flow pulsations due to a well-defined nozzle with a contraction ratio of 25, the flow was laminar at the nozzle exit. As is evident from Figure 4, the roll-up of the shear layer into discrete vortices is evident, with flow rapidly becoming turbulent within less than a diameter downstream of the nozzle exit. The spanwise coherency of the initial laminar instability waves is evident in Figure 4. Organization of the jet with upstream pulsations is quite evident in Figure 5. The nondimensional frequency fd/V_e was 0.3. It is clear from Figure 5 that the organization was axisymmetric. Looking at the spacing of these vortices in the jet, it was concluded from Figure 5 that these vortices converted at the mean velocity with spacing $\lambda/d = 1.1$ where λ is the spacing between the vortices.

The changes in the entrainment of the jet with and without primary jet pulsations were obtained by visualizing the entrained fluid marked by CO_2 gas. A slit of CO_2 gas was introduced at the jet spreading angle all along the jet. Typical results showing the instant behavior of the entrained fluid without and with pulsatile jets are shown in Figures 6 and 7 respectively. Figure 7 indicates a sharp interface between the entrained fluid and the organized vortex structure in the jet. From a close look at the entrained fluid, in Figure 7 as compared to Figure 6, it is inferred that the bulk of entrainment occurs at localized regions of the jet and shear layer for a pulsatile jet as compared to a nonpulsatile jet.

3.2. Influence of Pulsations on Free-Jet Growth

Typical hot-wire anemometry output results of the longitudinal velocity fluctuations are shown in Figure 8. The results obtained by traversing two hot wires relative to each other at a fixed distance from the nozzle and by looking at the phase of the velocity fluctuations showed that the pulsations were axisymmetric in nature.

To determine the influence of the pulsations of the jet on its growth, extensive mean velocity profile measurements were made at various axial locations downstream of the nozzle exit. These measurements were made at a fixed nozzle exit Mach number $M_{exit} = 0.2$ and over a range of pulsation frequencies from 0 to 1500 Hz. Two linearized constant temperature hot wires were employed to make the mean and the fluctuating velocity components measurement in the jet. One wire was fixed and located in the jet at $X/d = 0.5$ and was utilized to control the amplitude of free-jet pulsations. The second wire was traversed across the jet at various axial locations to measure the mean velocity U and the velocity fluctuations u' normal to the wire.

Before performing the detailed experiments, the performance of the nozzle was checked by computing the ideal thrust for an isentropic expansion given by $T_{isentropic} = \gamma M_e^2 p_\infty A_e$ as compared to directly measured thrust. Over the range of Mach numbers up to $M_{exit} = 0.7$, the nozzle efficiency defined by $T_{measured}/T_{isentropic}$ was more than 96%.

The influence on the free-jet growth rate of the pulsation frequency is shown in Figure 9 for various nondimensional frequencies fd/U_e. These results were obtained for a series of mean velocity profiles taken at various axial locations X/d at a fixed Mach number $M_{exit} = 0.2$. Throughout these experiments, the rms value of the longitudinal velocity fluctuations $\overline{u'^2}/U_e$ was kept at 10% at the nozzle exit. The decay of centerline velocity in the

present experiments at low nondimensional frequency of excitation (fd/U_e < 0.05) does not seem to influence the growth of the free jet. For fd/U_e > 0.05, the influence of excitation increases the decay of the centerline velocity. Present results further showed this enhanced decay to be independent of the pulsation frequency, at least within the accuracy of the present experimental results.

The above results were further supported when the influence of various pulsation frequencies on mean velocity profile growth and jet entrainment were determined, as shown in Figures 10 and 11. Up to X/d = 14, as discussed above, the growth of the jet and its entrainment at low pulsation frequency were not influenced by the pulsations.

3.3. Ejector Performance

Before determining how the entrainment and mixing of the entrained fluid with the primary jet influences the ejector performance, conservation of the jet momentum at various downstream locations was undertaken. The ratio of momentum (or thrust ratio) at a given station X was normalized with the one obtained at the nozzle exit. The profiles of the mean velocity, as obtained with the hot-wire anemometry, were utilized in these calculations. Typical results are shown in Figures 12 to 17 for nonpulsatile and pulsatile jets at various frequencies of jet flow pulsations. The Mach number at the nozzle exit was kept at M_e = 0.2. As is evident from the results shown in Figures 12 to 17, the momentum (or thrust) of the jet was conserved within an accuracy of 20% or less, which was considered satisfactory because of the limitation of hot-wire to measure accurately the velocity on the outer edge of the jet flow for the present investigation. It should be noted that in the above calculations no attempt was made to incorporate the momentum contributed by the fluctuating component flow.

3.3.1 Thrust Measurement

Typical results showing the influence of nozzle exit velocity on ejector performance are shown in Figure 18. Results of thrust measurements without upstream pulsations have been normalized with the corresponding thrust obtained without the presence of the ejector. Also indicated are the results obtained by pulsating the flow at a frequency of 500 Hz with nozzle exit velocity of about $U_e \approx 160$ m/s. A gain of approximately 14% for the steady ejector thrust was obtained. Table 2 shows similar results obtained with the ejector located at one primary nozzle diameter downstream from the nozzle exit plane.

For a fixed $M_e = 0.5$, the influence of the frequency of pulsations on ejector thrust performance is shown in Table 3. As can be seen, except at very low frequencies of pulsations ($fd/U_e < 0.03$), the thrust augmentations did not depend upon the frequency of oscillations. These results are consistent with the mean velocity data shown in Figures 9, 10 and 11. But for a fixed frequency of pulsations, the gain in thrust critically depends upon its amplitude as shown for various exit Mach numbers M_e in Table 4. A gain of as high as 15% in thrust augmentation from that obtained under steady flow conditions was obtained.

One of the major concerns throughout this investigation was the variation of the base primary jet thrust one observes with pulsations. To clarify this aspect, the influence of velocity fluctuations on thrust measured for the primary jet without ejector as well as the ejector performance with and without the pulsations was measured. The results of this finding are shown in Figure 19. The shaded area shows the gain in the thrust augmentation over and above that observed by a steady ejector flow where the gain in base primary jet thrust due to pulsations has been taken into account. As will be

discussed in the following section, this gain in thrust was related to the enhanced entrainment obtained due to the presence of pulsations in the primary jet flow.

3.3.2 Entrainment Results

To determine the relationship of thrust augmentation to enhanced entrainment for pulsatile jets as discussed above in section 3.3.1, mean velocity measurements were made at the ejector exit plane. By integrating the mean profile, the mean volume flow rate was computed. The ratios of the ejector volume flow rate normalized with the mean primary flow rate for pulsatile and nonpulsatile primary flow are tabulated in Table 5. Also indicated is normalized thrust T/T_0 where T_0 is the primary jet thrust. It is quite evident from these results that gain in thrust is accompanied by measured entrainment in the ejector system.

3.3.3 Pressure Distribution

Since the gain in thrust for pulsatile jet flow is accompanied by improvement in the entrainment by the ejector, pressure distribution measurements along the ejector wall were made to get further insight into the mechanism by which this entrainment was achieved. The pressure coefficient $C_p = \frac{P - P_\infty}{1/2\rho U_e^2}$ was measured at various selected positions as indicated on Figure 30. The present results indicate that, with pulsations, large improvement in creating pressure below atmospheric pressure was achieved. This will result in improved entrainment because of reduced pressure as observed in this investigation. It is inferred from these results that the entrainment is closely related to the reduced pressure on the inlet geometry of the ejector. As will be disucssed in Section 3.3.6, this is why inlet flow plays a key role in ejector performance.

3.3.4 Ejector Length and Area Ratio Effects

For a given area ratio, i.e., D/d = 3.5, and primary flow Mach number M_e = 0.2, influence of the length of the ejector on its performance was determined for various lengths of the ejectors. The typical results of this finding are shown in Figure 21. As is evident in Figure 21, for L/D = 1.71, very little thrust augmentation was achieved. For L/D = 3.65 and 6.86, improvement in ejector performance weakly depended upon the frequency of pulsations as shown in Figure 22. But for a given length L/D = 3.65, when the area ratio was modified, i.e., D/d, marked changes (up to 14% gain in thrust over steady state value) in ejector performance were observed when the pulsations were introduced. There were regions of frequencies over which this improvement in performance was observed, indicating a dynamic coupling of the ejector flow system. The details of various geometries utilized to determine the area and length effects on ejector performance are given in Table 1.

3.3.5 Diffuser Effects

As with area ratio effects, improvement in thrust performance was observed with an ejector which had a constant area ejector followed by a diffuser. The length of the diffuser was such that in both cases the flow was expanded to the same area ratio, which in the present case was an increase of 46% in area from that of the constant area ejector. A gain as high as 14% over steady-state ejector performance was observed in these measurements (Fig. 23). For details of the geometry the reader should refer to Table 1.

3.3.6 Inlet Effects

Preliminary experiments were performed to determine the influence of inlet geometry on ejector performance and entrainment. The typical results are shown in Figures 24 and 25. The results were compared for no inlet, a flat plate inlet, and a hemispherical nose of two sizes. The lucite nose had D' = 7.0", whereas the wooden nose diameter D' = 12.0" (see sketch in Table

1). The experimental results in Figure 24 indicate the importance of the inlet flow (suction capability as discussed in section 3.3.3) in thrust augmentation. The corresponding gain in the entrainment as measured at the ejector exit plane further supports the close relationship of the entrainment to the performance of the ejector.

IV. CONCLUSIONS

The present investigation clearly demonstrated the importance of entrainment in augmentation of the thrust of an ejector. Since this entrainment can be improved by ejector design, active fluid controls, pulsated primary flow, etc., there is a great potential to design a compact and efficient ejector. The principal conclusions of pulsatile ejector flow results are as follows:

1. Ejector thrust performance can be improved by as much as 15% over the steady-state peformance.
2. Thrust augmentation critically depended upon the amplitude of pulsations and was independent of its frequency.
3. Inlet flow conditions play an important role in ejector performance.
4. Enhanced augmentation in pulsatile ejector flows resulted in:
   a. Lower pressure (improved suction) at the inlet of the ejector.
   b. Enhanced entrainment by the ejector flow system.

ACKNOWLEDGEMENTS

This report presents the results of one phase of research carried out at the Jet Propulsion Laboratory, California Institute of Technology, Contract NAS7-100, Task Order RD-182, Amendment 63, sponsored by the Naval Air Systems Command under MIPR No. N00019-80-MP-07850. The authors extend their gratitude to Prof. M. F. Platzer, U. S. Naval Postgraduate School, Monterey, California,

for many valuable technical suggestions throughout this program. The authors are grateful to Mr. P. F. Massier for his continuous encouragement and technical advice. The assistance of Mr. Stan Kikkert for design, fabrication and the assembly of the experimental setup is greatly appreciated.

REFERENCES

1. Quinn, B., "Compact Ejector Thrust Augmentation," J. of Aircraft, Vol. 10, No. 8, August 1973, pp. 481-486.
2. Von Karman, T., "Theoretical Remarks on Thrust Augmentation," Reissner Anniversary Volume Contributions to Applied Mechanics, J. W. Edwards, Ann Arbor, Michigan, 1949.
3. Bevilagua, P. M., "Analytical Description of Hypermixing and Test of an Improved Nozzle," J. of Aircraft, Vol. 13, No. 1, January 1976, pp. 43-48.
4. Salter, G. R., "Methods for Analysis of V/STOL Aircraft Ejectors," J. of Aircraft, Vol. 12, No. 12, December 1975, pp. 974-978.
5. Bevilagua, P. M., "Evaluation of Hypermixing for Thrust Augmenting Ejectors," J. of Aircraft, Vol. 11, No. 6, June 1974, pp. 348-354.
6. G. Binder and M. Favre - Marinet "Mixing Improvement in Pulsating Turbulent Jets" in Fluid Mechanics of Mixing (ed. Uram and Goldschmidt), ASME United Engineering Center, 1973, pp 167-172.
7. Bremhorst, K. and Harch, W.H., "Nearfield Velocity Measurements in a Fully Pulsed Subsonic Air Jet", in Turbulent Shear Flows I ed. by Durst, F., Launder, B.E., Schmidt, F.W., and Whitelaw, J.H., Springer-Verlag, Berlin, Heidelberg, 1979, pp 37-54.
8. Crow, S. C. and Champagne, F. H., "Orderly Structures in Jet Turbulence," J. of Fluid Mechanics, Vol. 48, 1971, pp. 547-591.
9. P. Leister, "Experimental Investigation on the Turbulence of an Impinging, Pulsating Jet," Paper presented at the Symposium on Turbulent Shear Flows, April 18-20, 1977, at University Park, PA.

10. M. F. Platzer, J. M. Simmons, and K. Bremhorst, "On the Entrainment Characteristics of Unsteady Subsonic Jets," AIAA Journal, Vol. 16, March 1978, pp. 282-284.

11. I. Wygnanski, D. Oster, B. Dziomba and H. Fiedler, "On the Effect of Initial Conditions on Two-Dimensional Turbulent Mixing Layer," Journal of Fluid Mechanics, 1979, Vol. 93, p. 325.

Table 1 - Dimensions of the Ejector System

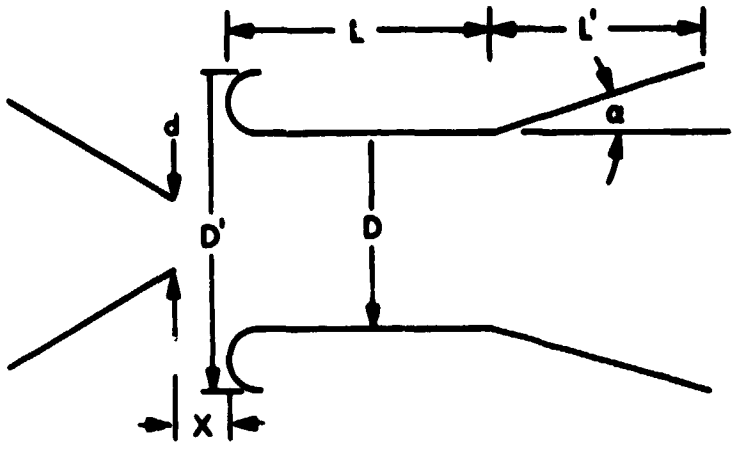

d = 2.54 cm and D = 17.8 cm for constant area ejector system measurements.

Area Ratio Effects

$\frac{L}{D}$ = 3.4 (fixed)

Varied $\frac{D}{d}$ = 2, 3.5 and 5

Ejector Length Effects

$\frac{D}{d}$ = 3.5 (fixed)

Varied $\frac{L}{D}$ = 1.7, 3.4, 6.9

Diffuser Effects

Constant area ejector $\frac{L}{D}$ = 3.4 and $\frac{D}{d}$ = 3.5 (fixed)

Varied L' = 15.2 cm, α = 3.5° and L' = 7.6 cm, α = 7°

These dimensions gave a 46% increase in the area of the diffuser exit as compared to the constant area ejector.

Table 2 - Ejector Performance at Various Exit Mach Numbers

X/d = 1.0

M_{exit}	$T_{ejector}/T_o$
0	1.0
0.07	3.56
0.11	1.375
0.17	1.275
0.22	1.23
0.26	1.24
0.30	1.23
0.34	1.22
0.38	1.22
0.42	1.21
0.45	1.21
0.50	1.20
0.53	1.20
0.56	1.20
0.60	1.20
0.63	1.19
0.66	1.20
0.70	1.19

Table 3 - Influence of the Frequency of Pulsations on Ejector Performance

$M_e = 0.50$

$X/d = 1.0$

Frequency of Pulsations	$\frac{fd}{U_e}$	$\overline{u'^2}/U_e$	$T_{ejector}/T_o$
0	0	0.01(Random)	1.2
50	.007	0.08	1.22
100	0.015	0.08	1.21
200	0.03	0.08	1.22
300	0.046	0.06	1.28
400	0.062	0.08	1.30
500	0.08	0.08	1.24
600	0.09	0.08	1.27
700	0.10	0.08	1.30
800	0.12	0.08	1.26
900	0.14	0.06	1.28
1000	0.17	0.03	1.25
1100	0.17	0.03	1.26
1200	0.19	0.02	1.24
1300	0.20	0.02	1.22
1400	0.217	0.02	1.27

Table 4 - Influence of the Amplitude of Velocity Pulsations on Ejector Performance

Frequency of Pulsations = 500 Hz

Ejector Located at X/d = 1.0

M_e	$\overline{u'^2}/U_e$	fd/U_e	$T_{ejector}/T_o$
0.1	0.01	Random	1.1
0.1	0.10	0.4	1.2
0.1	0.20	0.4	1.2
0.2	0.01	Random	1.15
0.2	0.1	0.2	1.21
0.2	0.15	0.2	1.24
0.2	0.21	0.2	1.27
0.3	0.01	Random	1.15
0.3	0.05	0.12	1.17
0.3	0.10	0.12	1.23
0.3	0.17	0.12	1.27
0.4	0.01	Random	1.16
0.4	0.05	0.09	1.17
0.4	0.10	0.09	1.22
0.4	0.17	0.19	1.27
0.5	0.01	Random	1.16
0.5	0.05	0.07	1.21
0.5	1.10	0.07	1.31

Table 5 - Influence of Pulsations on Entrainment

Frequency of Pulsations 500 Hz

M_e	$\overline{u'^2}/U_e$	Q/Q_o	T/T_o
0.3	0.01 (without pulsations)	3.94	1.15
0.3	0.05	4.04	1.17
0.3	0.10	4.64	1.23
0.3	0.17	4.50	1.27
0.5	0.01 (without pulsations)	14.8	1.16
0.5	0.05	15.5	1.21
0.5	1.1	16.8	1.31

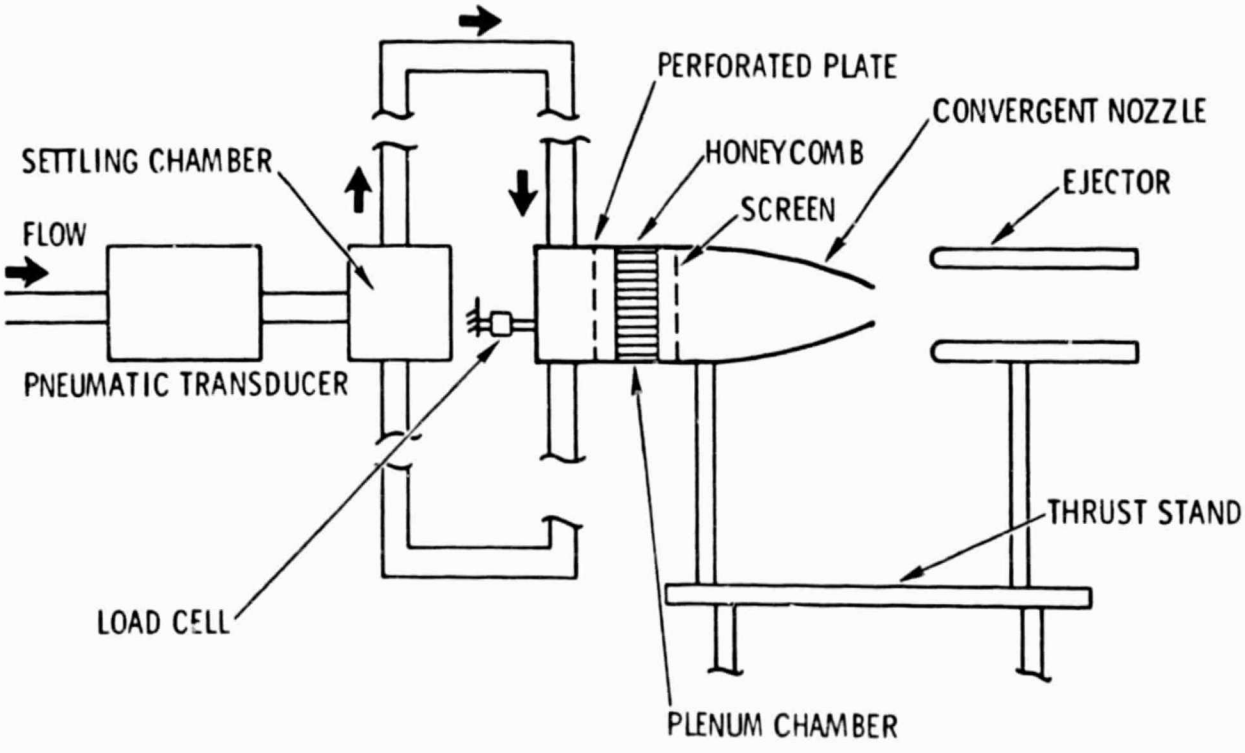

Figure 1. Schematic Diagram of Thrust Augmentor.

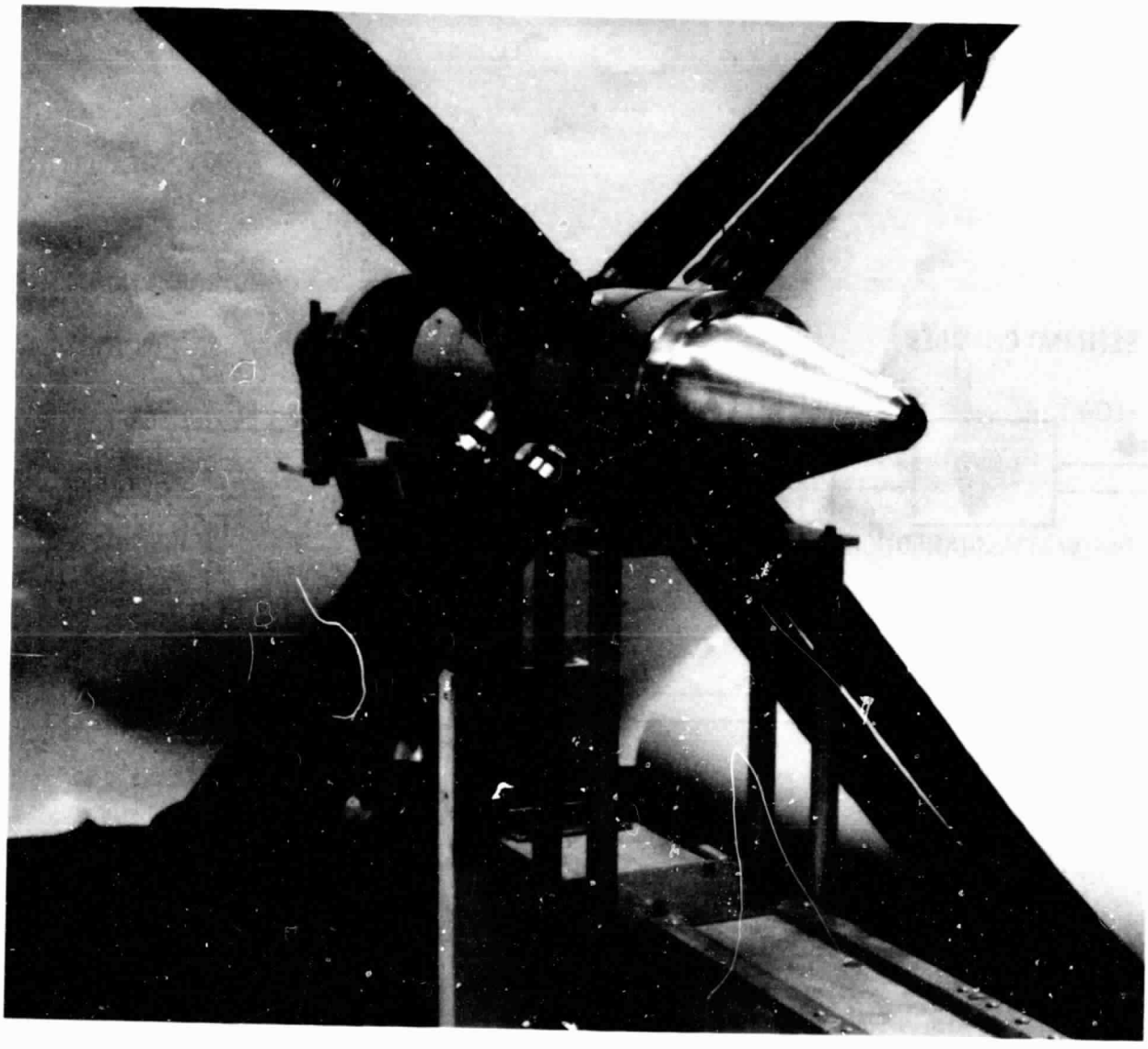

Figure 2. Primary Nozzle Flow Experimental Arrangements.

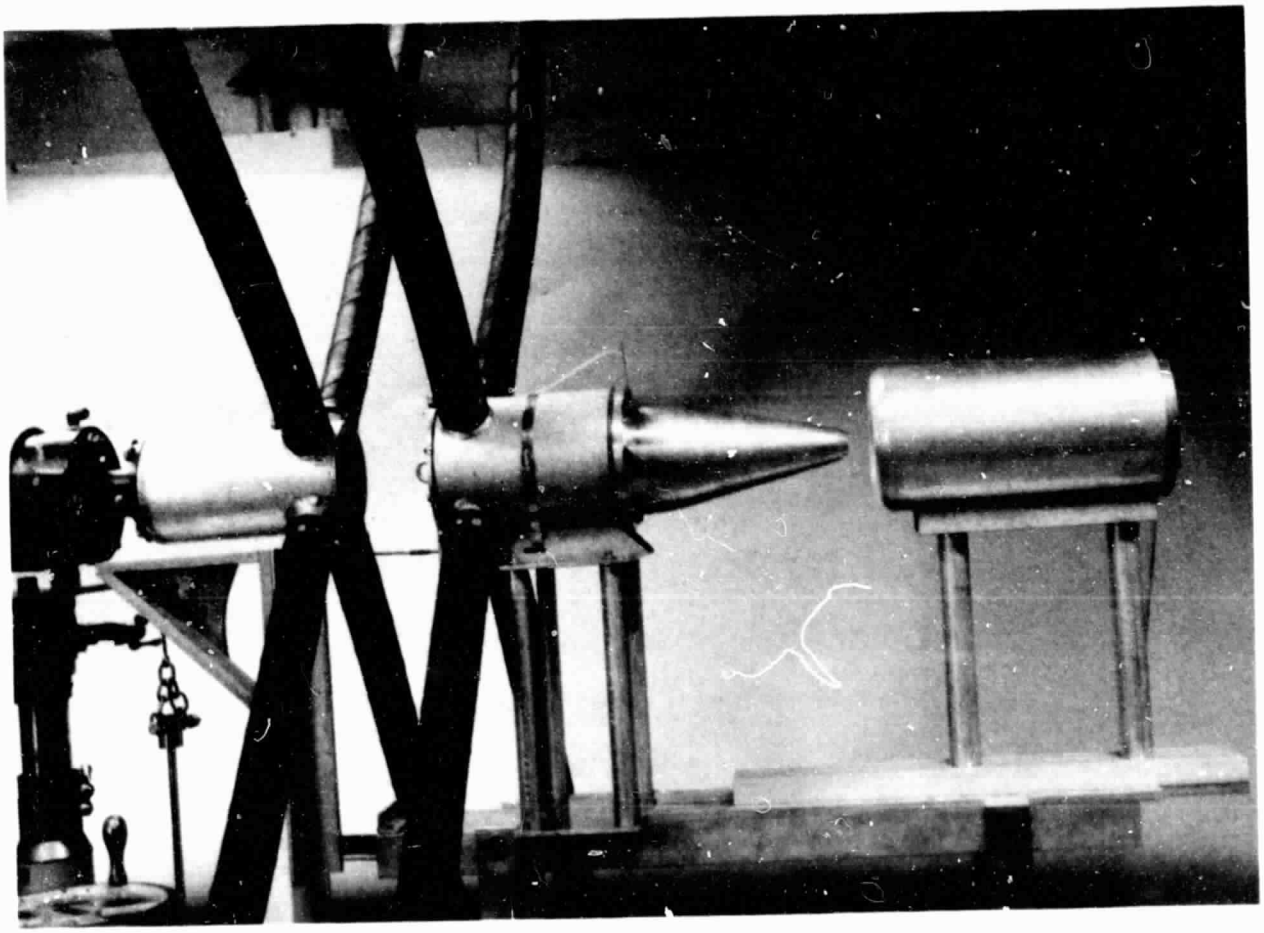

Figure 3. Primary Flow and Constant-Area Ejector.

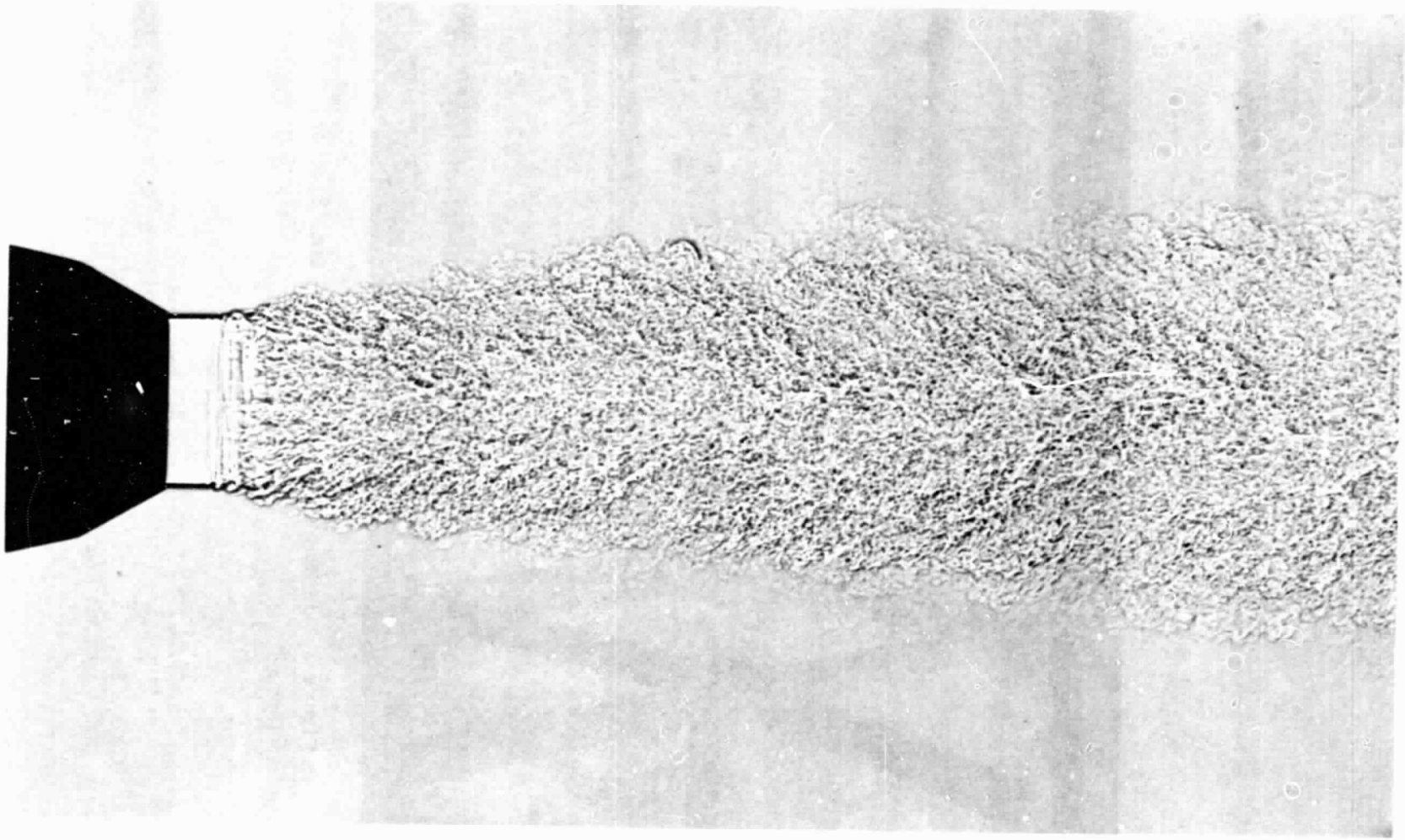

Figure 4. Subsonic Jet Exhausting Into Ambient Air Without Upstream Pulsations. Velocity at Nozzle Exit = 52 m/s.

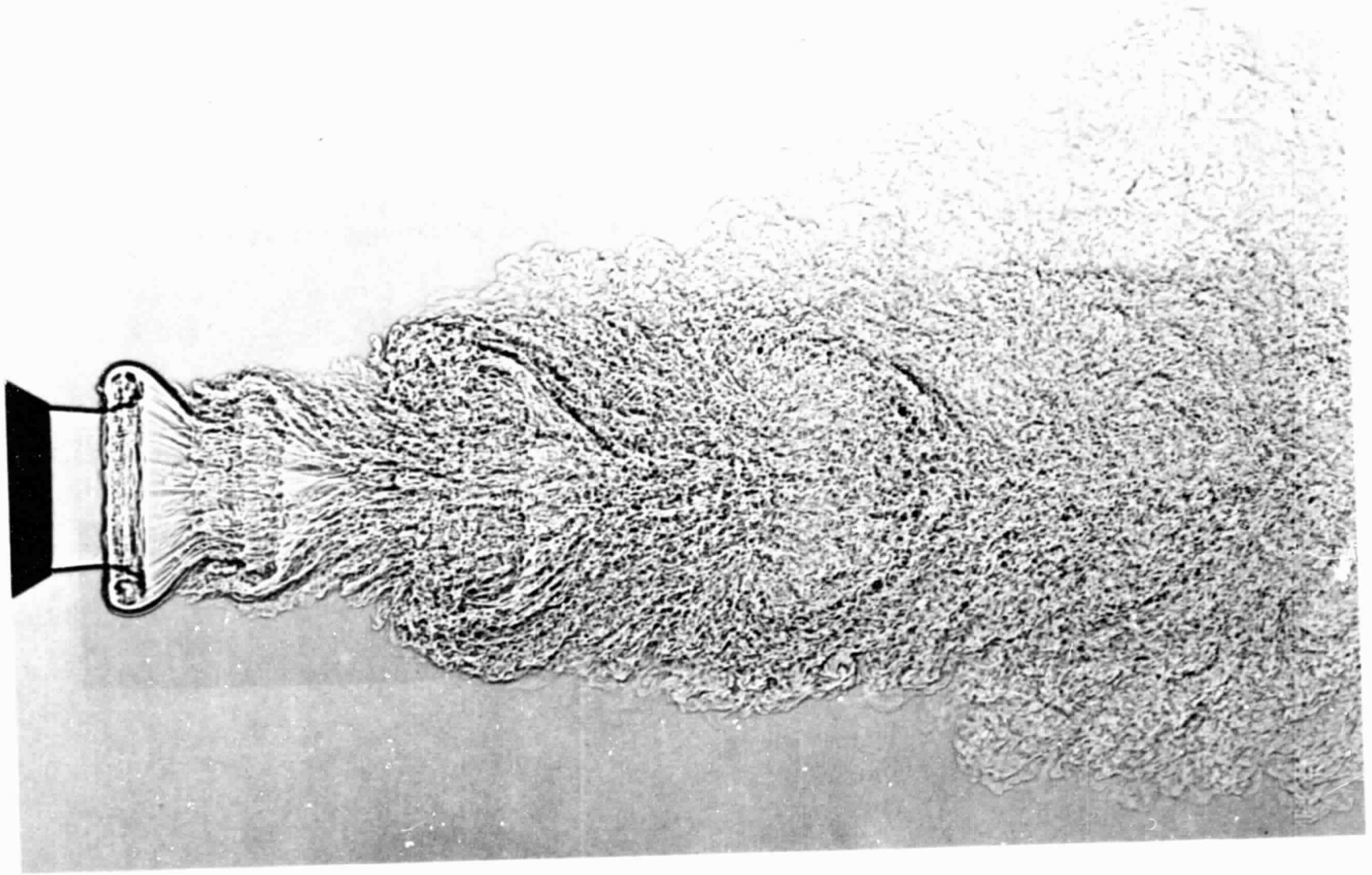

Figure 5. Subsonic Jet Exhausting Into Ambient Air With Upstream Pulsations. Velocity at Nozzle Exit = 52 m/s. Frequency fd/U_e = 0.3.

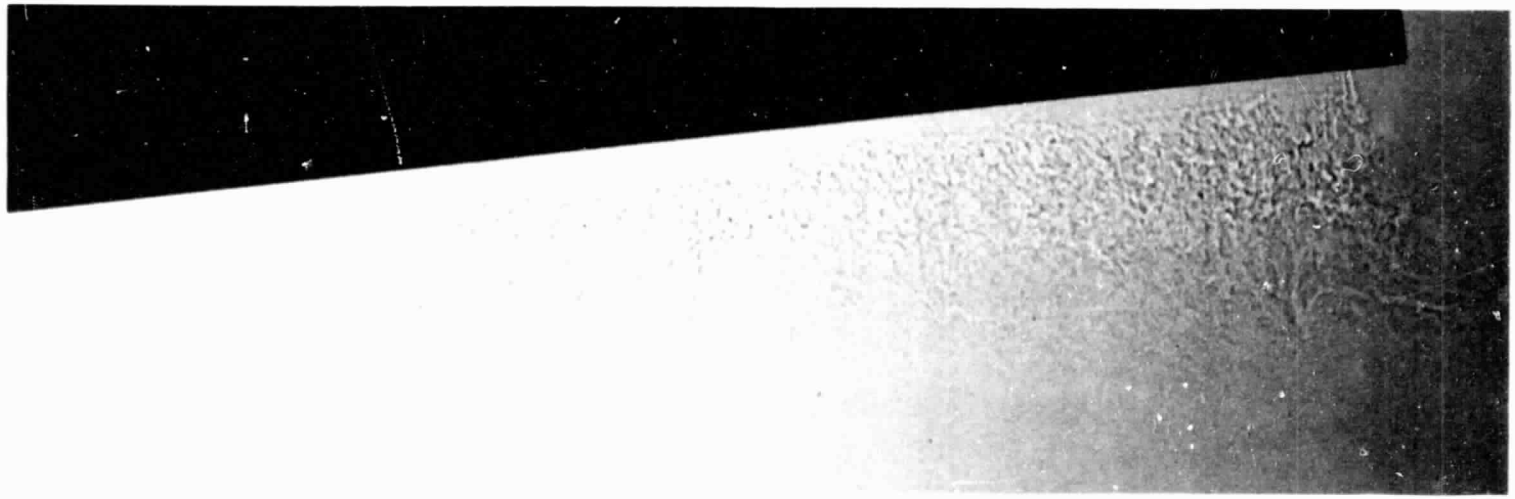

Figure 6. Shadowgraph Showing Entrained Flow of a Jet. Velocity at Nozzle Exit = 152 m/s.

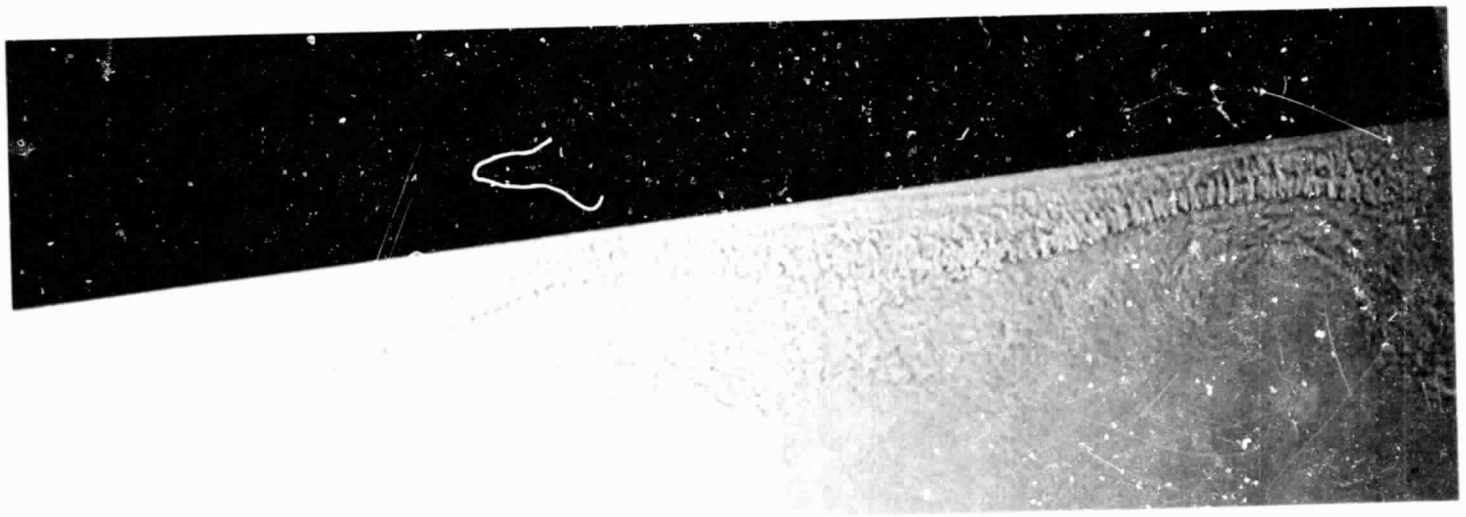

Figure 7. Shadowgraph Showing Entrained Flow of a Pulsed Jet. Nozzle Exit Velocity = 152 m/s. Frequency fd/U_e = 0.07.

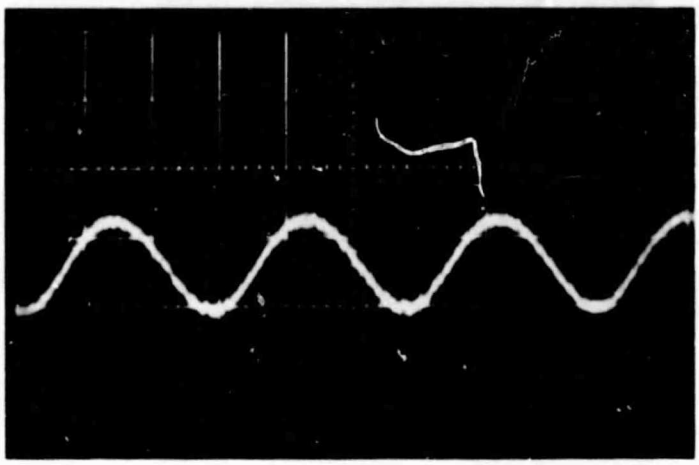

PULSATION FREQUENCY 136 Hz

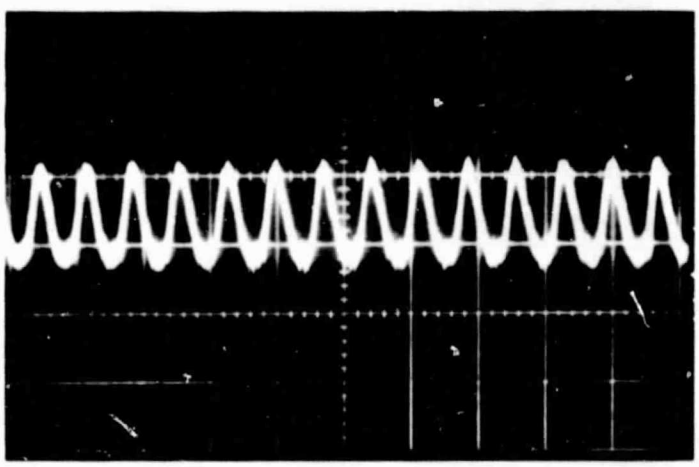

PULSATION FREQUENCY 546 Hz
HORIZONTAL SCALE 2 ms/division
VERTICAL SCALE 0.2 V/division

Figure 8. Linearized Constant Temperature Hot-Wire Anemometry Output.

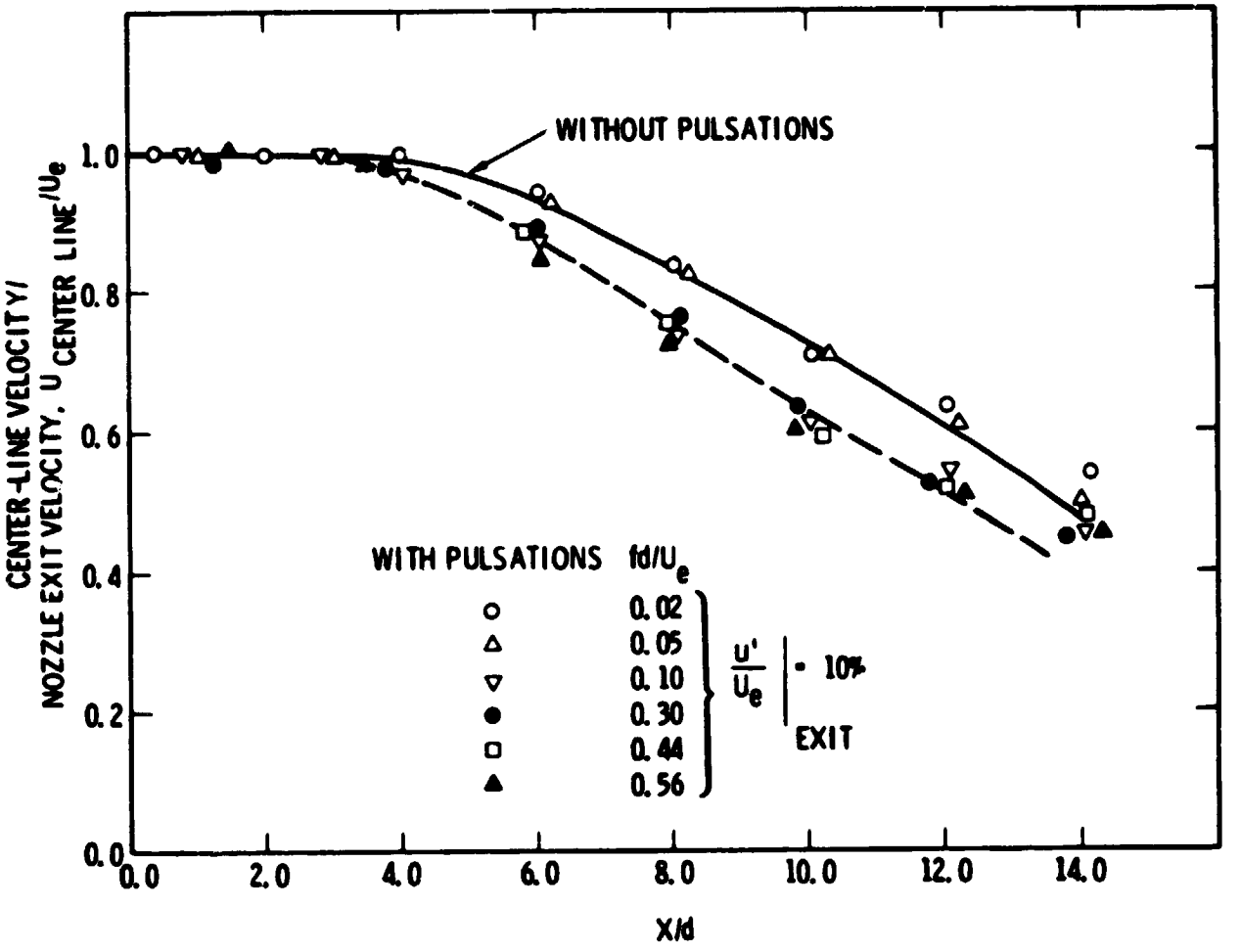

Figure 9. Centerline Velocity Decay.

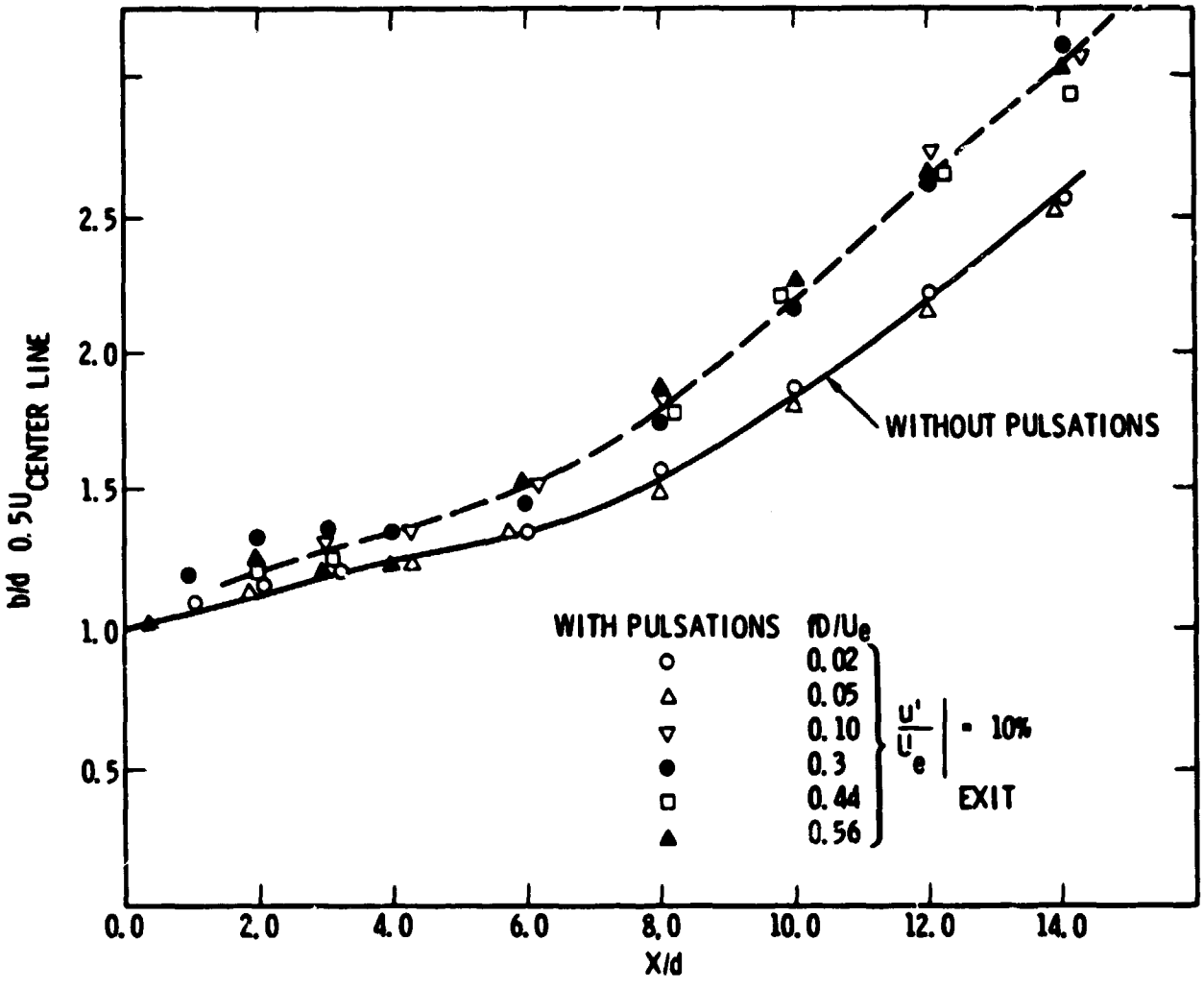

Figure 10. Growth of Jet.

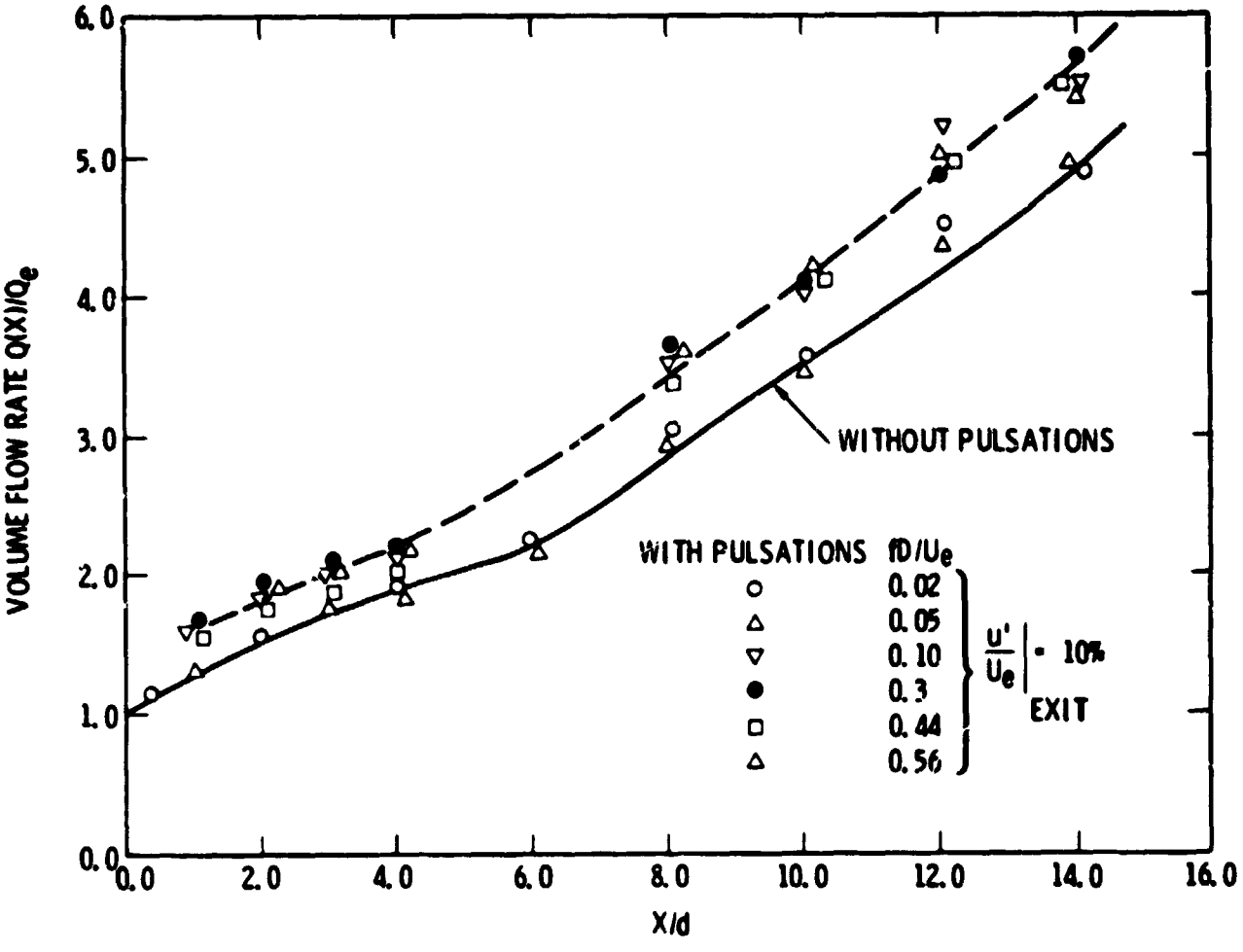

Figure 11. Entrainment of Flow by a Free-Jet.

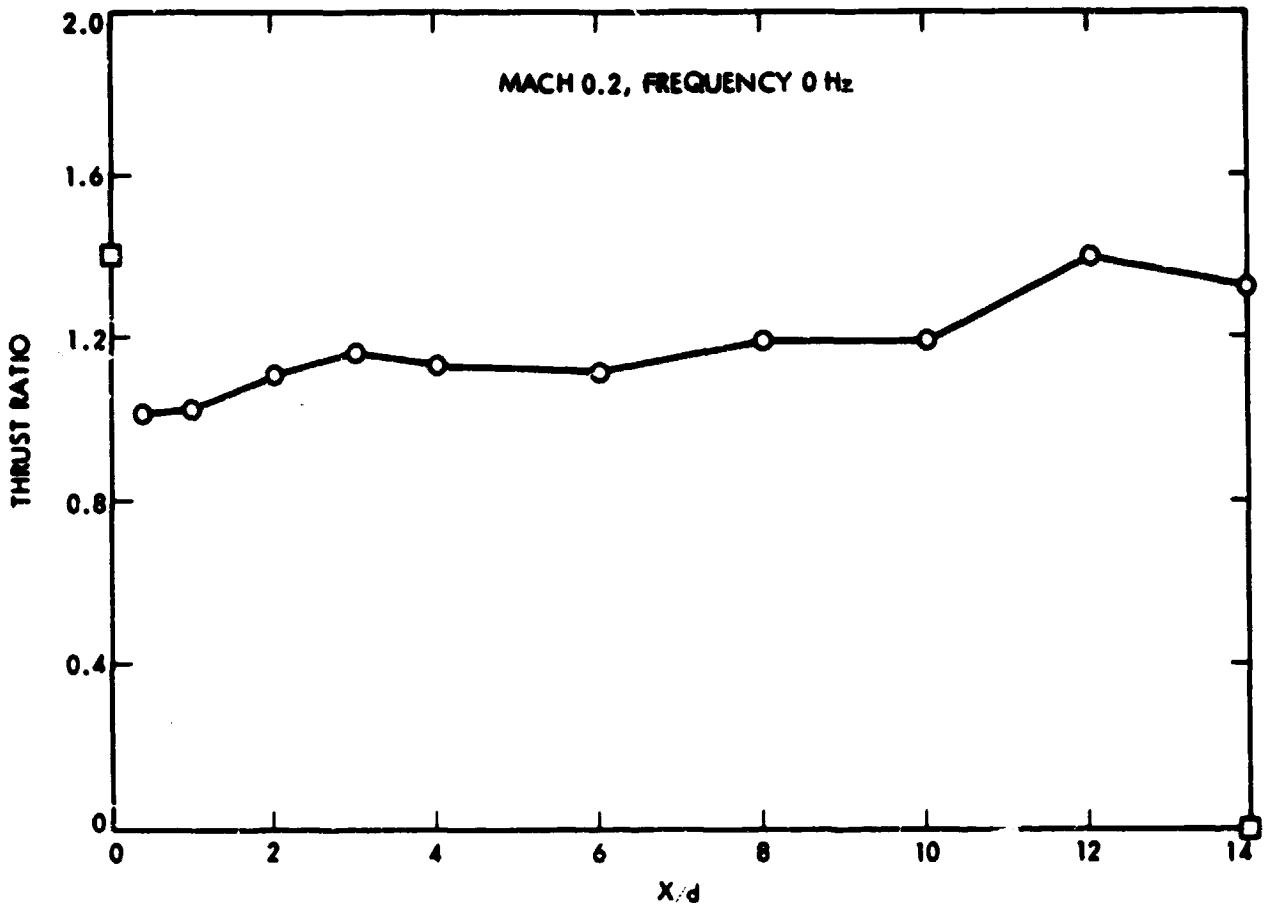

Figure 12. Conservation of Momentum/Thrust Without Pulsations.

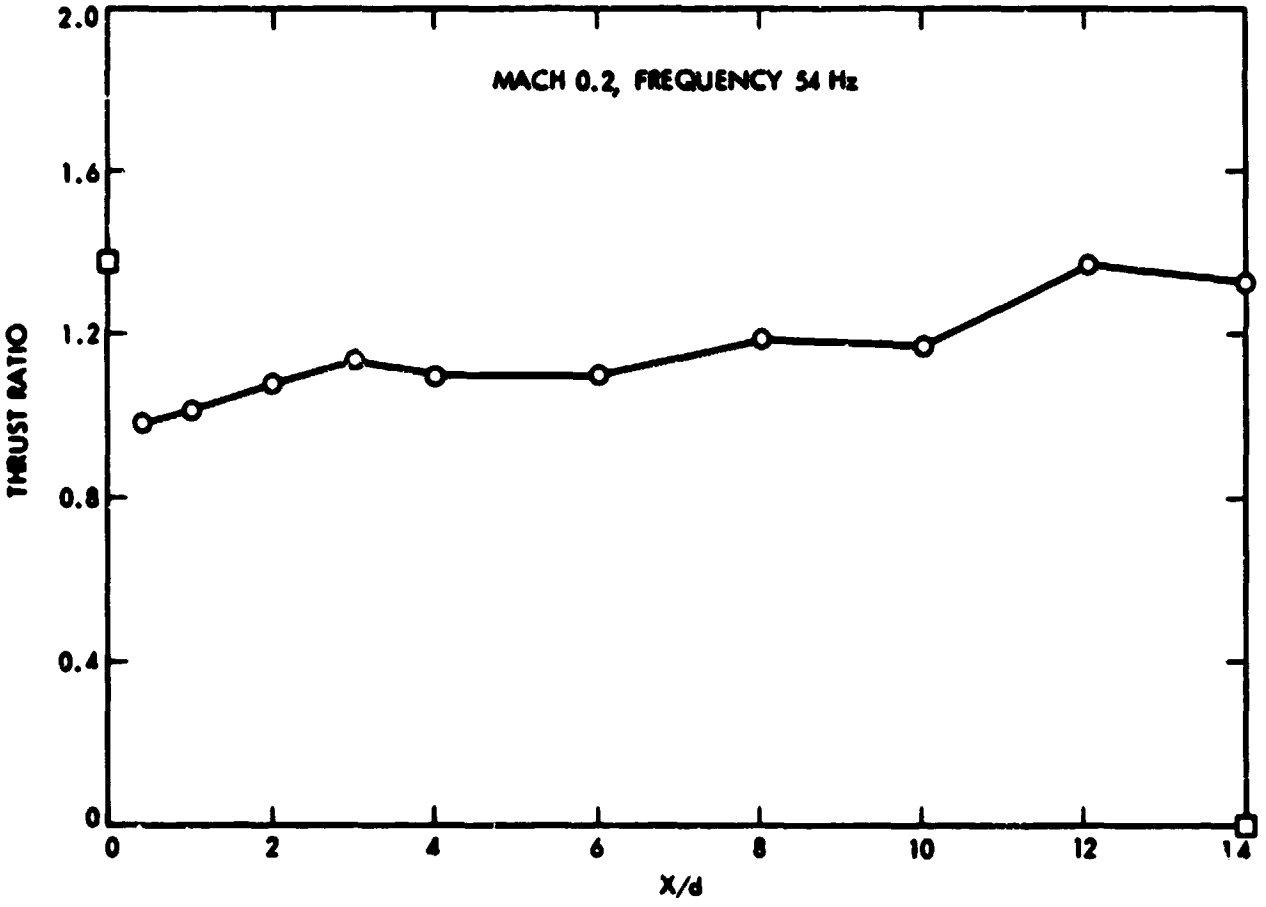

Figure 13. Conservation of Momentum/Thrust With Pulsations; f = 54 Hz.

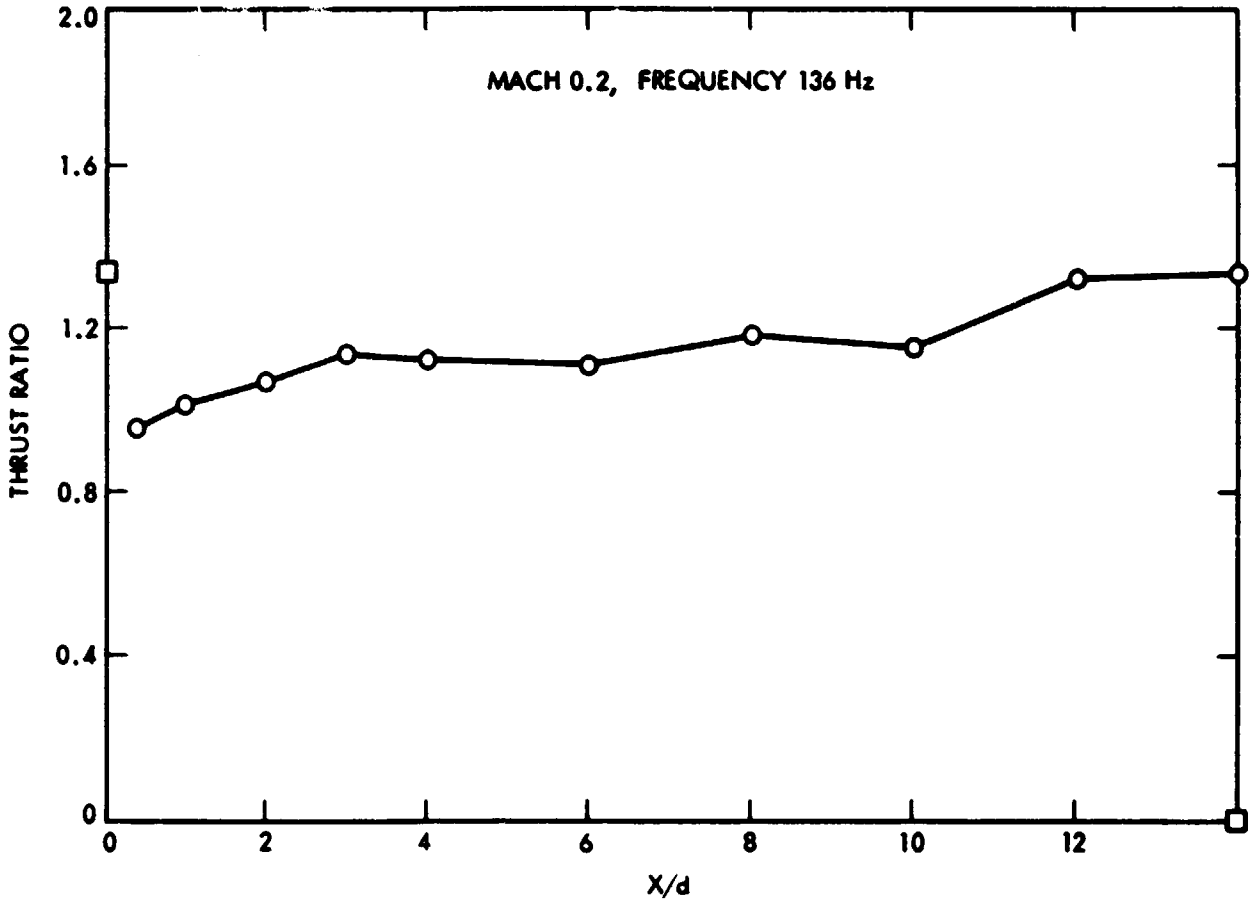

Figure 14. Conservation of Momentum/Thrust With Pulsations; f = 136 Hz.

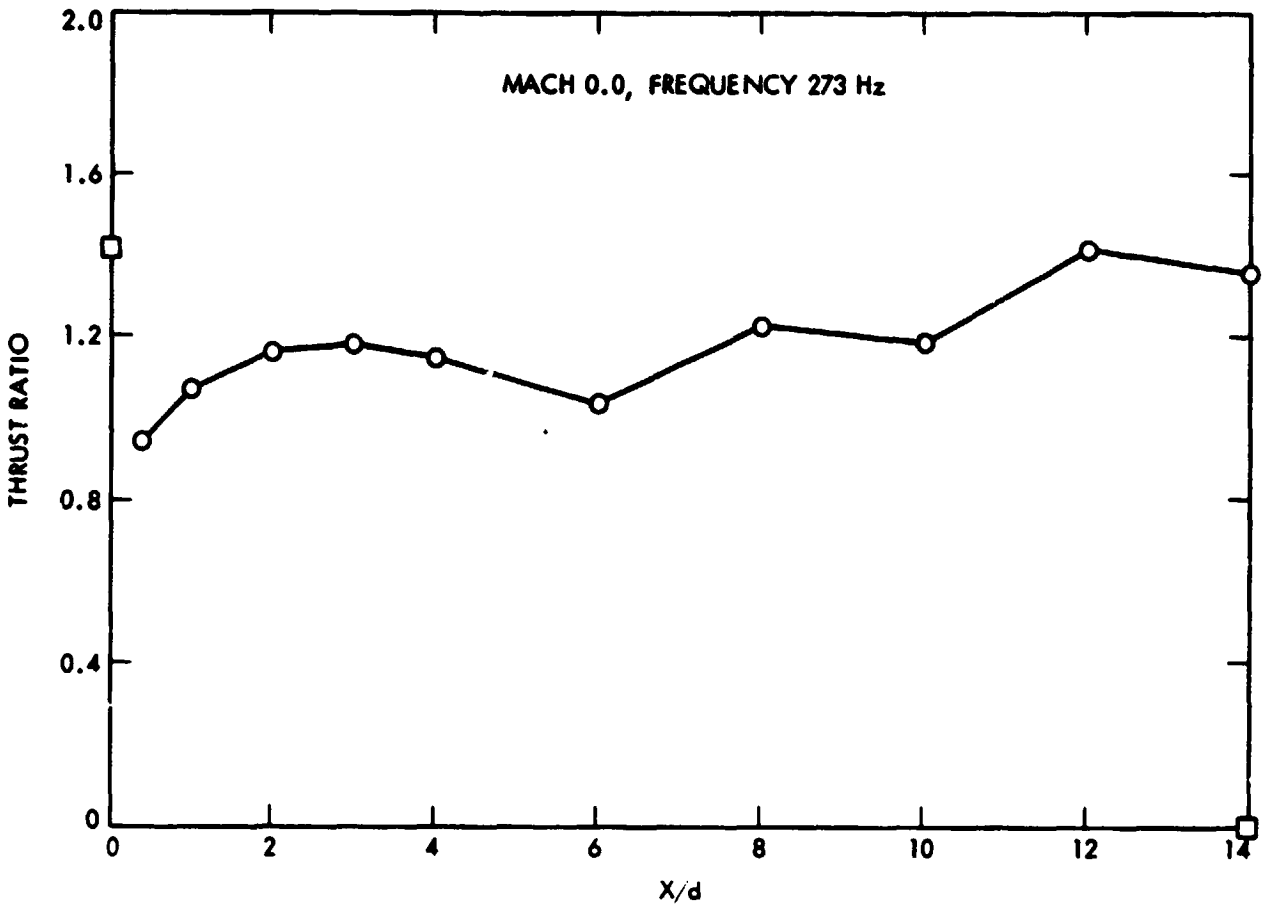

Figure 15. Conservation of Momentum/Thrust With Pulsations; f = 273 Hz.

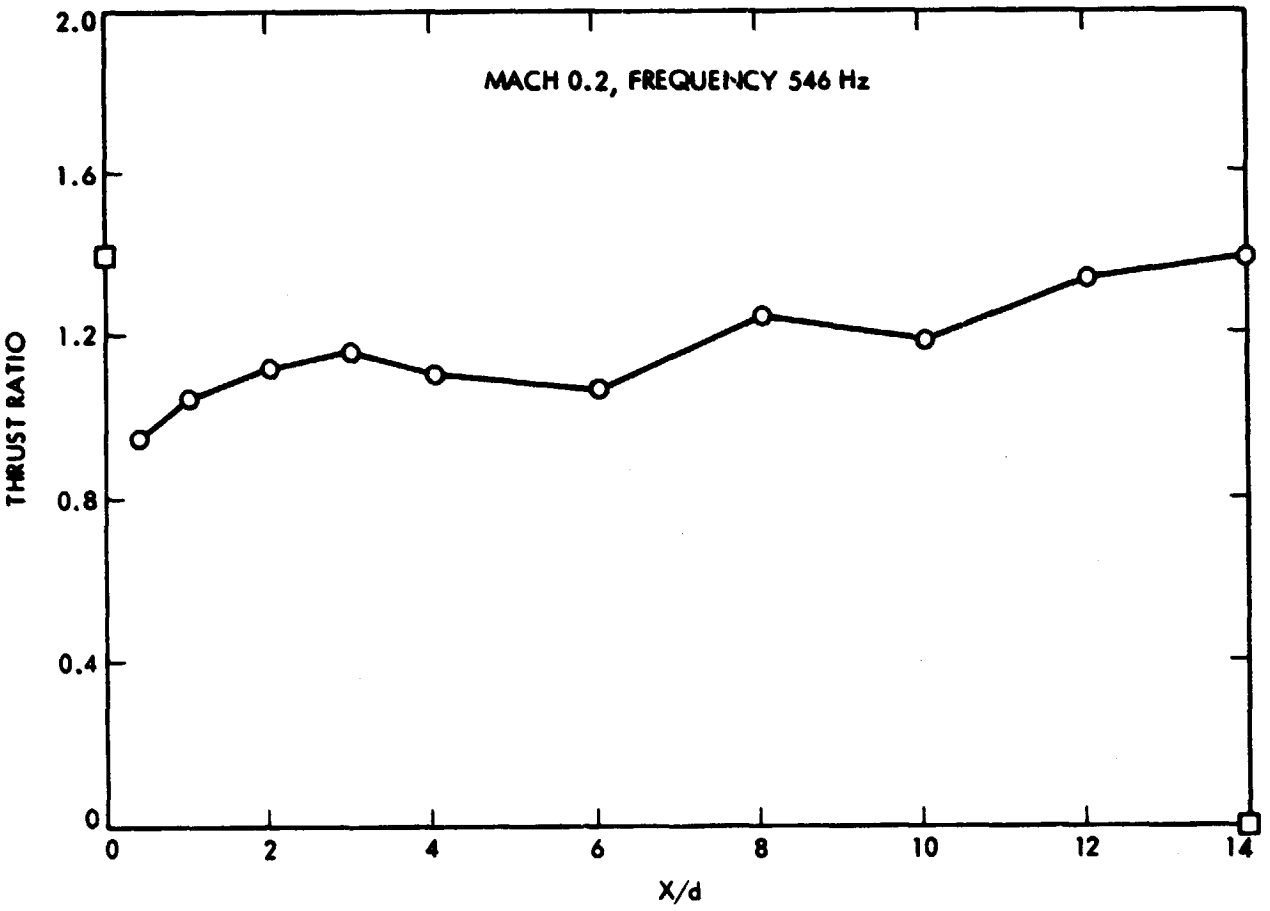

Figure 16. Conservation of Momentum/Thrust With Pulsations; f = 546 Hz.

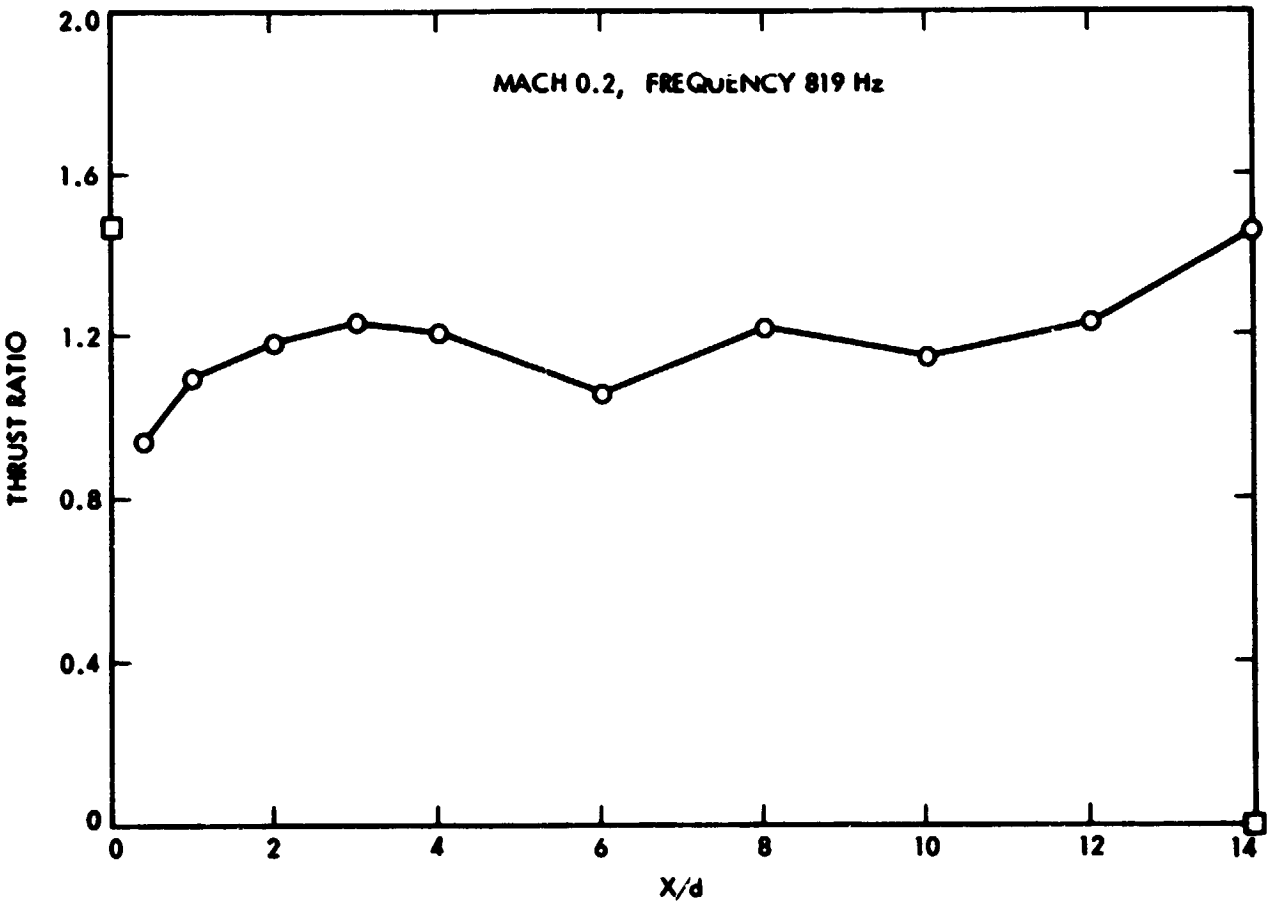

Figure 17. Conservation of Momentum/Thrust With Pulsations; f = 819 Hz.

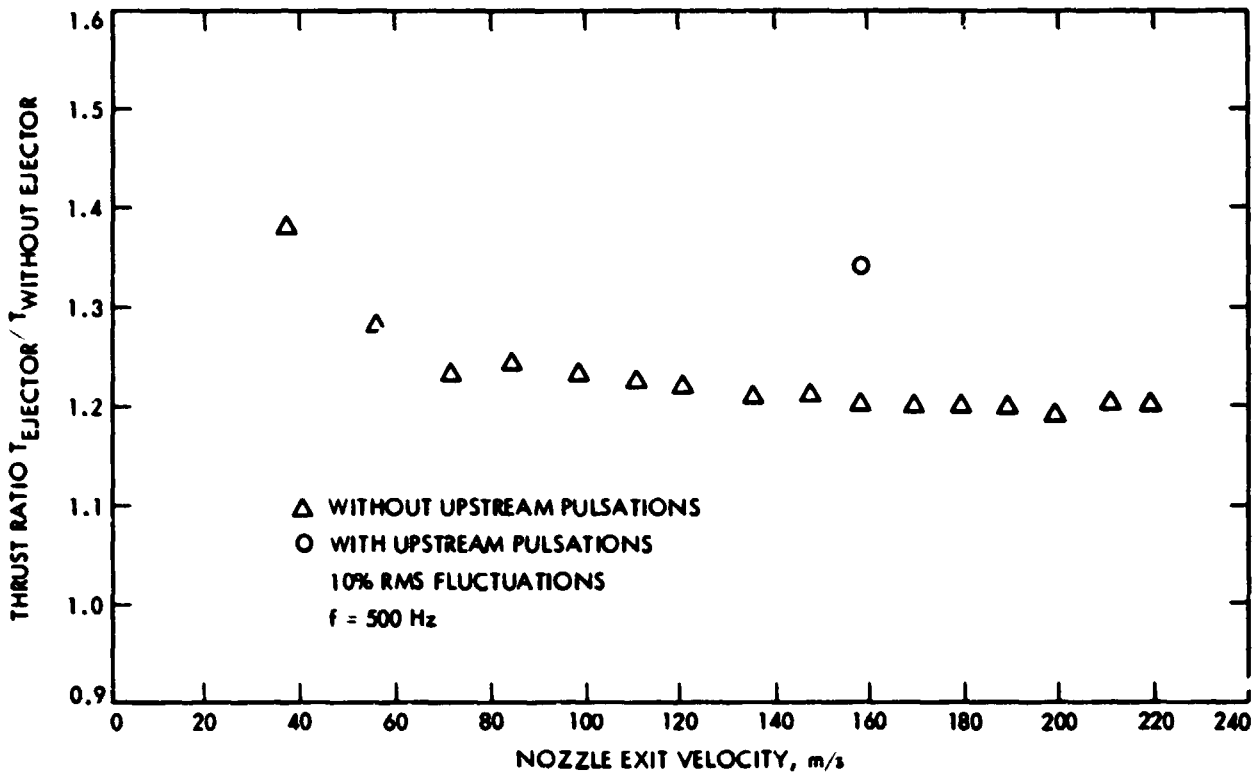

Figure 18. Thrust Augmentation of a Constant-Area Ejector.

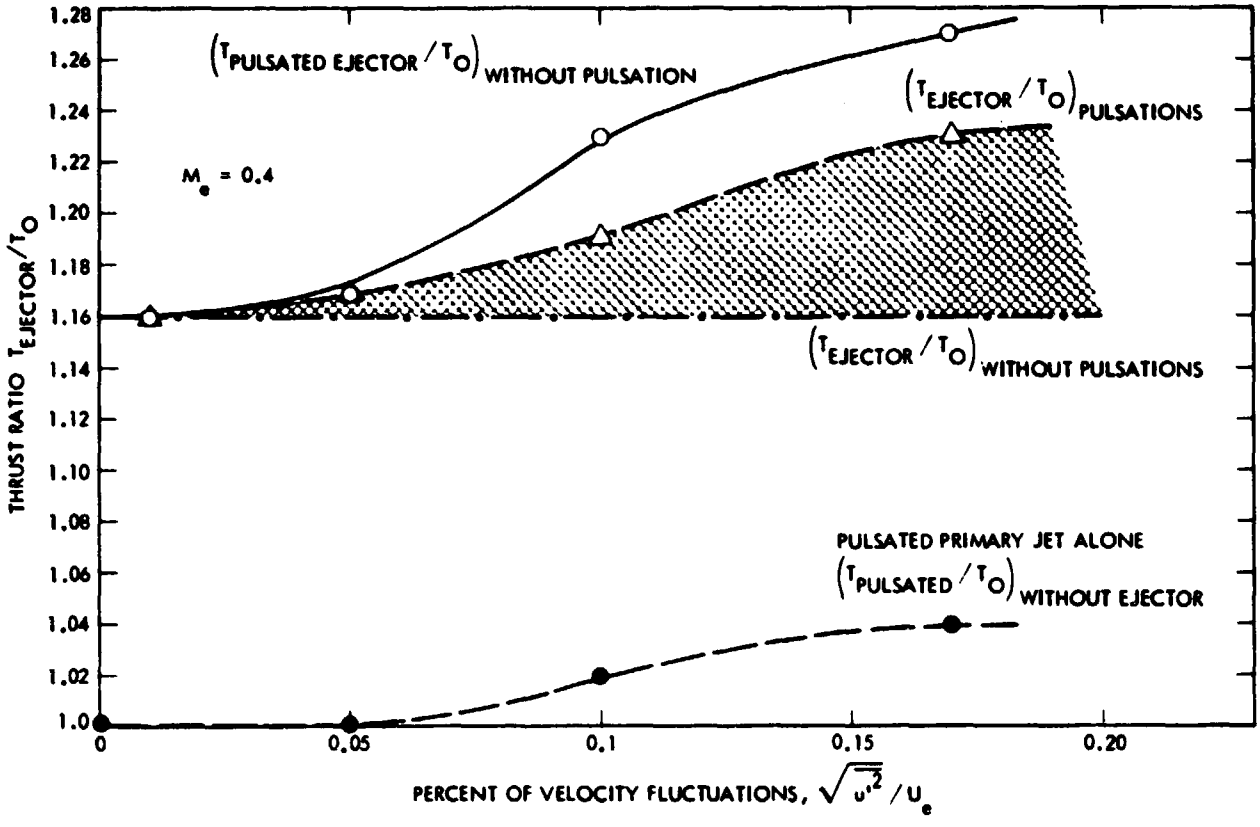

Figure 19. Influence of Amplitude of Velocity Fluctuations on Ejector Performance.

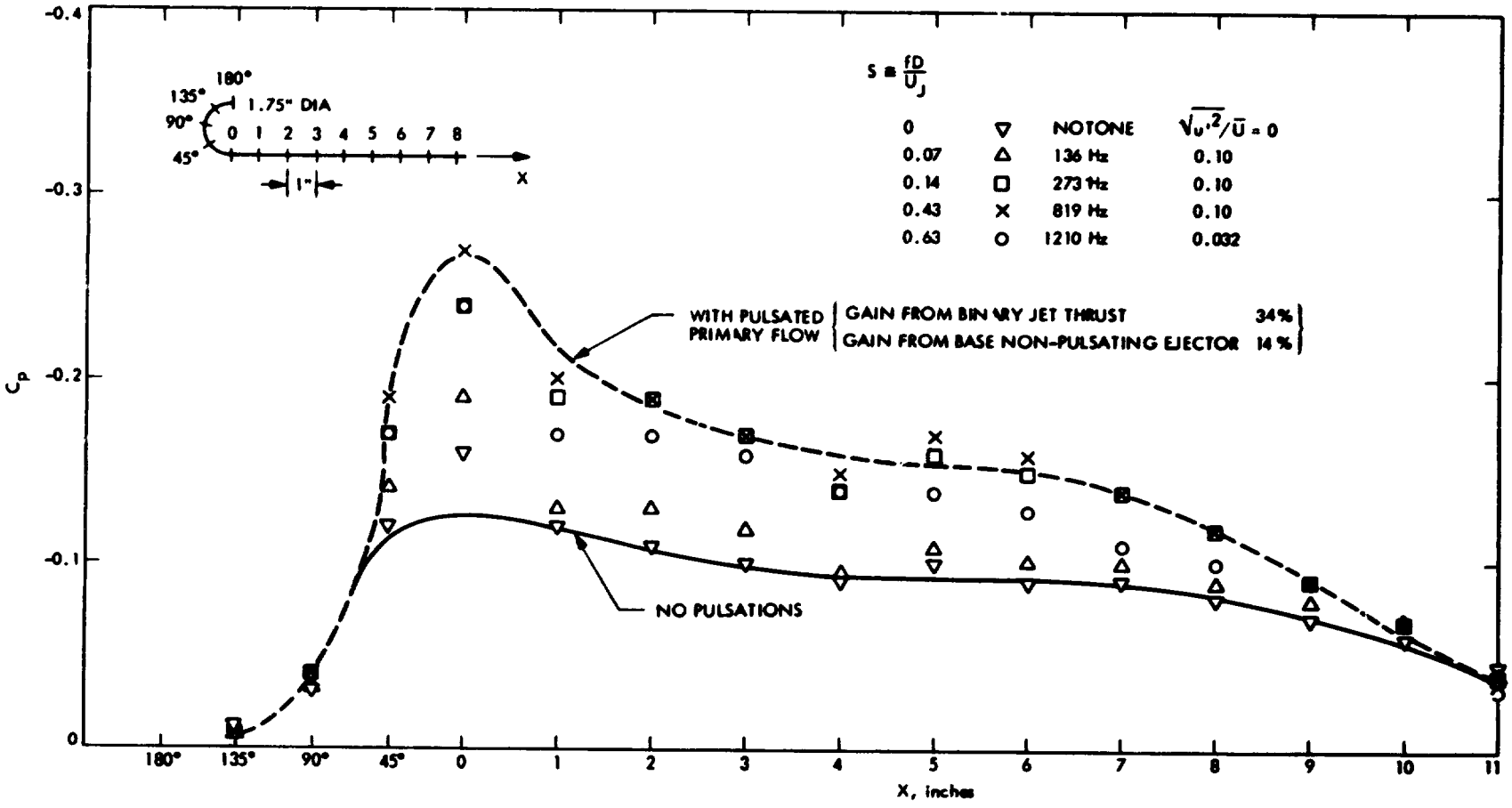

Figure 20. Pressure Distribution Along Ejector Wall With and Without Pulsating Primary Jet.

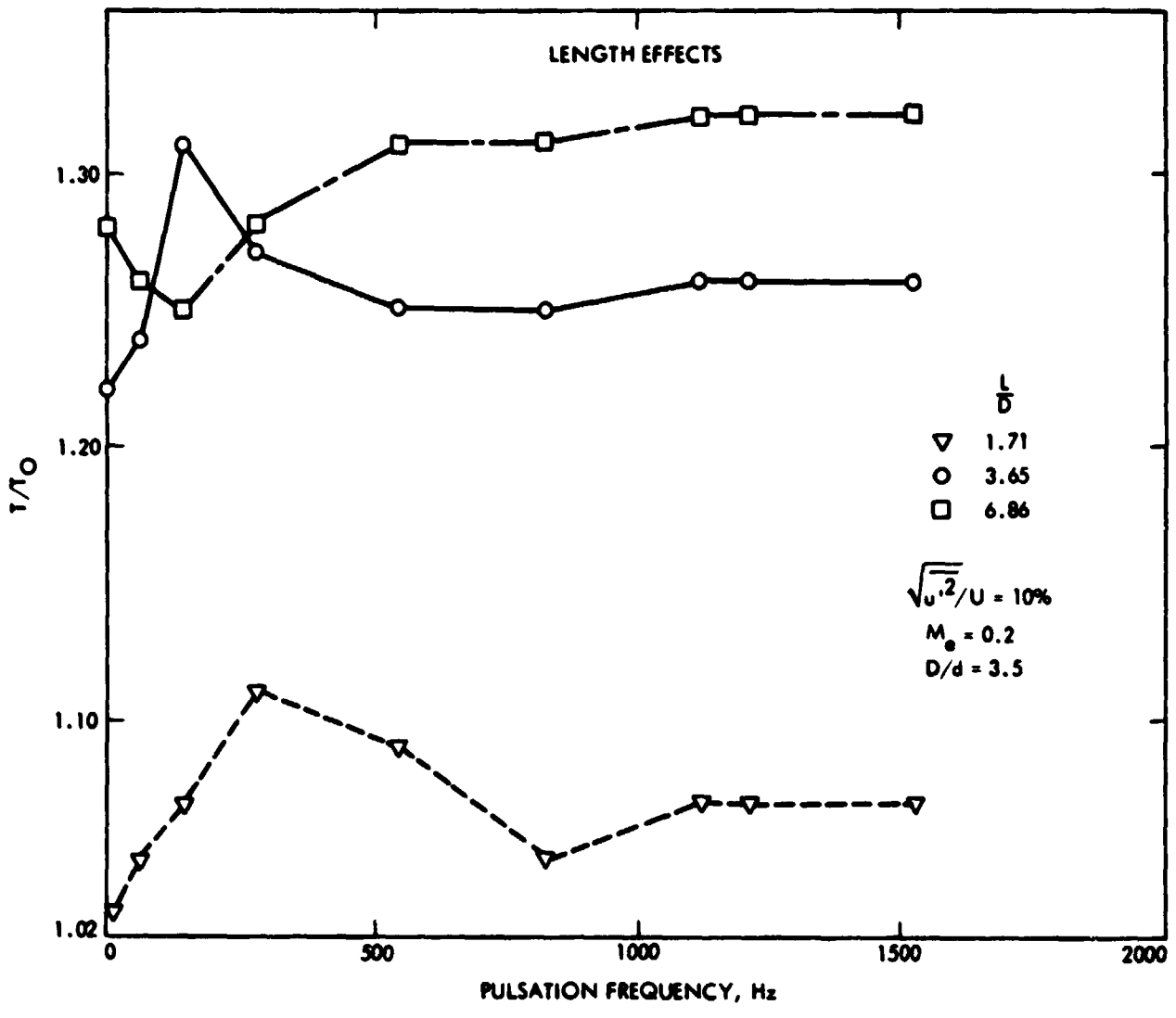

Figure 21. Influence of Pulsations on Ejector Performance.

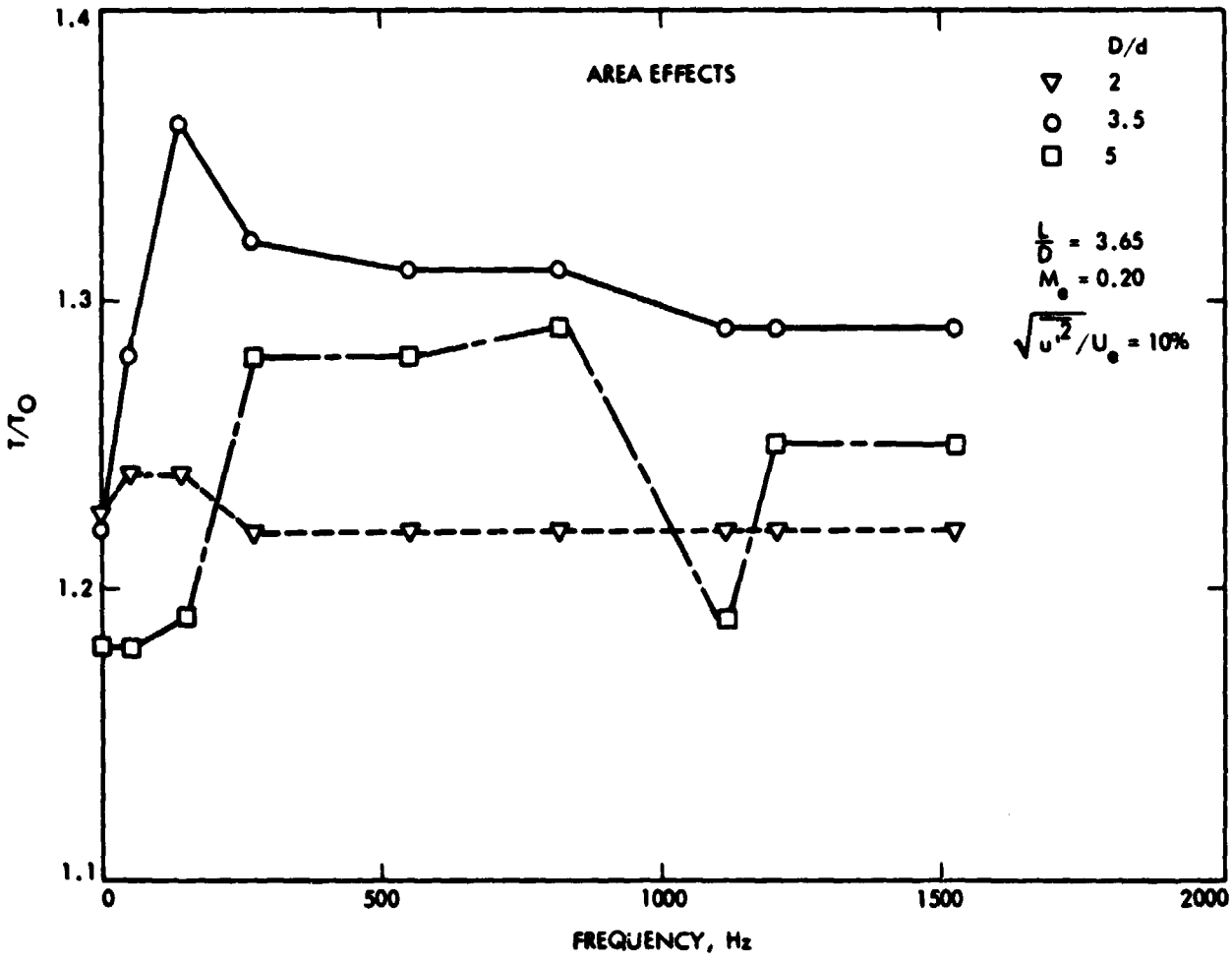

Figure 22. Effect of Pulsations on Ejector Performance.

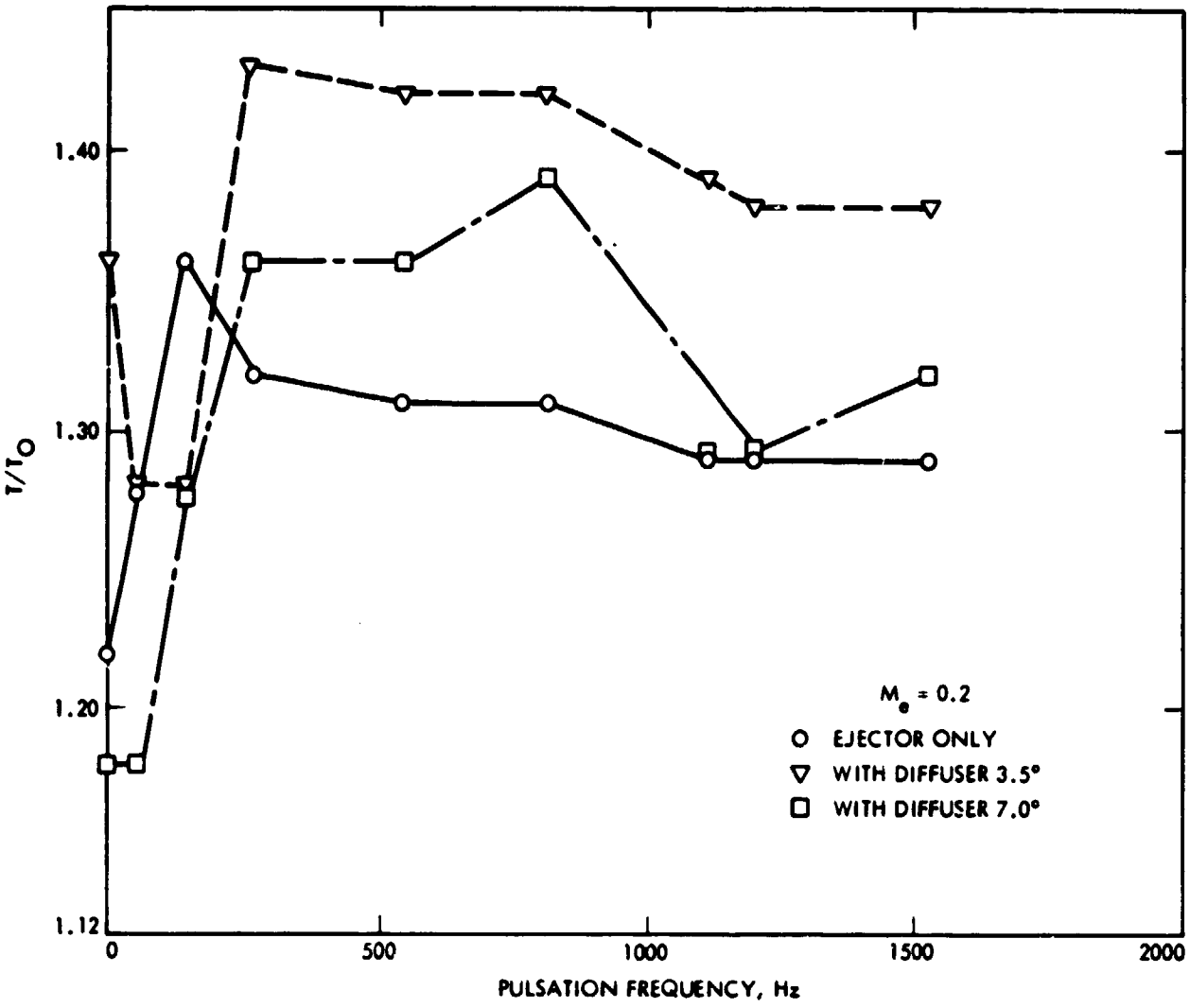

Figure 23. Effect of Pulsations on Ejector Performance with Diffuser.

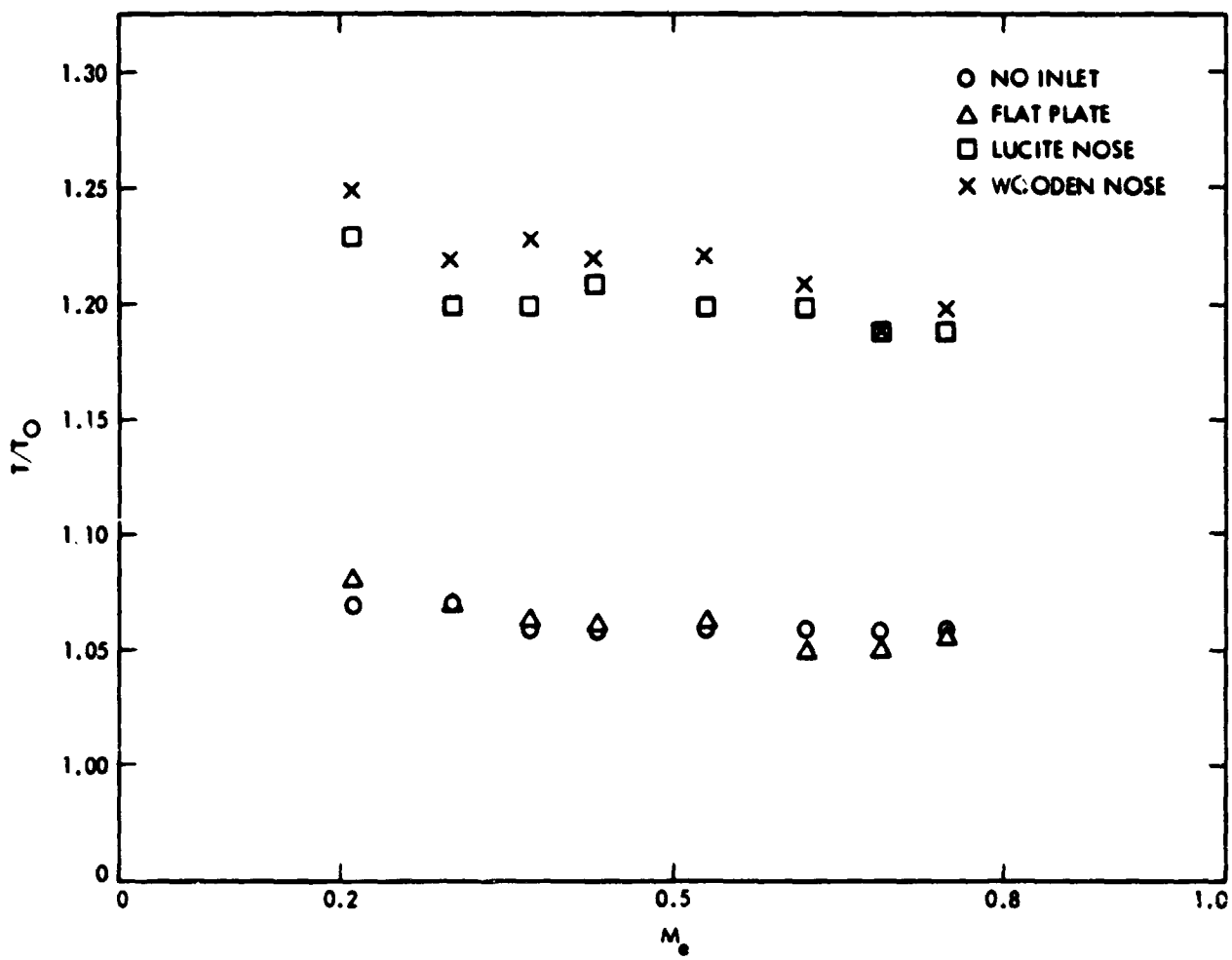

Figure 24. Ejector Inlet Effects.

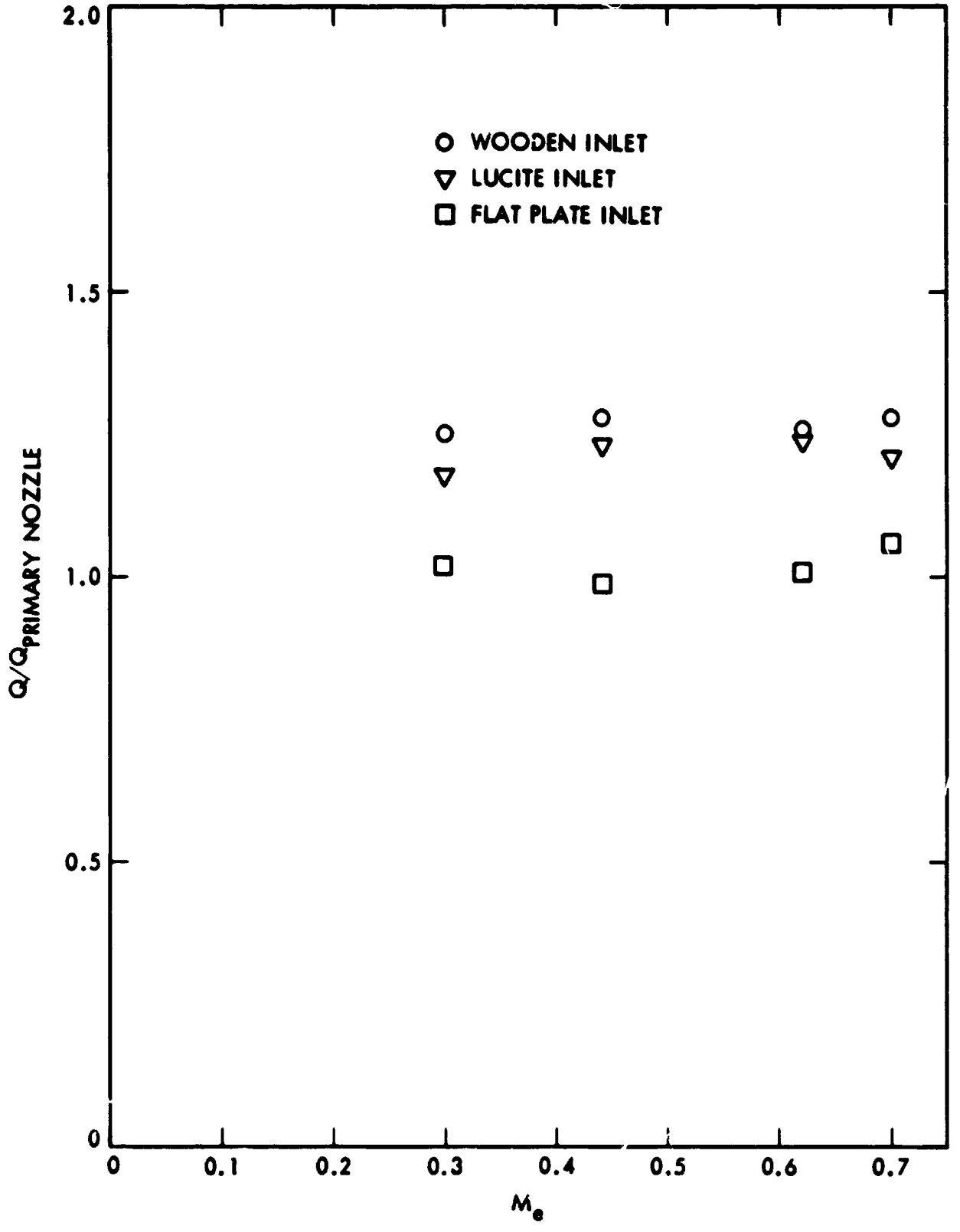

Figure 25. Influence of Ejector Inlet Flow on Entrainment